



NSW Nearshore Wave Tool Update

Offshore Wave Height Extreme Value Analysis

24 October 2024 | 12359.201.R2.Rev0

Baird.
Innovation Engineered.

baird.com

Prepared for:

Prepared by:



Department of Climate Change, Energy, the Environment and Water



Baird Australia Pty Ltd as Trustee for the Baird Australia Unit Trust
ACN 161 683 889 | ABN 92 798 128 010

12359.201.R2.Rev0

Z:\Shared With Me\QMS\2024\Reports_2024\12359.201.R2.Rev0_NSW_Nearshore_Waves_OffshoreEVA.docx

Revision	Date	Status	Comments	Prepared	Reviewed	Approved
0	2024-10-24	Final	Issued for Use	AB / SG	DT	DT

© 2025 State of NSW and Department of Climate Change, Energy, the Environment and Water All Rights Reserved.

DISCLAIMER: This report was prepared by Baird Australia Pty Ltd in good faith exercising all due care and attention, but no representation or warranty, express or implied, is made as to the relevance, accuracy, completeness or fitness for purpose of this document in respect of any particular user's circumstances. Users of this document should satisfy themselves concerning its application to, and where necessary seek expert advice in respect of, their situation. The views expressed within are not necessarily the views of the Department of Climate Change, Energy, the Environment and Water and may not represent department policy.



Baird's Quality Management System has been certified by Bureau Veritas against the requirements of ISO 9001.

Executive Summary

This report presents an analysis of the deepwater extreme wave (height) climate at the seven (7) deepwater wave buoy locations that form DCCEEW's long term wave measurement program.

Extreme value statistics, presented as Average Recurrence Interval (ARI), have been prepared based on the long term non-directional and directional wave measurement data for NSW (see Section 2.1.1), and the newly generated 67-year hindcast data set covering the period of 1957 to 2023 that has been generated for the NSW Nearshore Wave Tool (see Baird, 2024).

The extreme value data presented in the following sections employ statistical analysis methods and Peaks Over Threshold (POT) data censoring that is specifically tailored to generate the most appropriate return period estimates for each site and dataset. The processes and methods adopted for the Extreme Value Analysis (EVA) are described in Section 2.3, and the censoring and optimisation performed for the EVA results presented in this report are customised for each extreme value sample that has been analysed. As a result of the customised EVA methods being adopted in this study, the extreme value statistics presented in Section 3 of this report will likely differ than those that may be prepared with the same datasets using the automated EVA tools available in the online The NSW Nearshore Wave Tool (see Baird, 2024). The extreme value statistics presented in this report are considered more reliable than those generated by the automated EVA tools available in the online The NSW Nearshore Wave Tool as the POT value and fitting parameters have been optimised for each location and directional data set that is presented in this report.

The 67-year hindcast data set described in (Baird, 2024) has been extensively calibrated and validated to provide an improved validation to the NSW deepwater wave dataset as summarised in Section 2.1. That dataset has excellent validation in terms of the overall directional wave climate (hindcast model skill > 0.9, bias ± 0.1 m and RMSE error < 0.4 m), and extreme event statistics (see Section 3 and Appendix B), compared to the available historical deepwater wave datasets (see Section 2.1.1). The new longer-duration hindcast data set, in conjunction with refined extreme value analysis methods (see Section 2.3), has generated an improved understanding of the NSW deepwater extreme value climate compared to earlier studies including Shand *et al* (2011) and Glatz *et al* (2017). However, the analysis and definition of the directional extreme wave height climate is still limited by fewer storms in the northeast and east-southeast directional sectors which results in significantly more uncertainty in the extreme directional wave height climate compared to the omnidirectional condition.

Based on the limited offshore and nearshore wave data available from the 1970's, and earlier hindcasts of 1970 storm events (for example Taylor *et al*, 2017), it has been well recognised that the NSW wave climate for return periods of 50-years ARI and greater may be more severe than can be estimated from the available deepwater measured datasets or hindcast datasets that have been analysed to date. The most significant advancement in the definition of the NSW deepwater wave climate from this study is that significant storms that occurred between 1957 to 1979 are now appropriately represented in the longer duration wave datasets. In particular, the storms that occurred in the 1970's along the mid-NSW coast, including the May 1974, have resulted in a significant increase in the extreme wave height estimate for 20-years ARI and greater using the new 67-year deepwater hindcast data sets.

In addition to the increased estimates of extreme wave heights, the new 67-year deepwater hindcast datasets also improves the definition of the long-term directional wave climate, including the frequency and magnitude of storms that generate large wave heights from northeast to east offshore wave directions. However, there is significantly more statistical uncertainty in the definition of the extreme directional wave climate for northeast and east-southeast wave directions. Table E.1 provides a summary of the estimated deepwater omnidirectional wave heights (1-hour exceedance) based on the 67-year hindcast for selected ARI's for the seven offshore wave buoy locations operated programs funded by DCCEEW.

Table E.1: Summary of extreme 1-hour exceedance omnidirectional wave height for selected ARI's based on 67-year Baird (2024) hindcast. (Values in brackets denote the 95% confidence intervals.)

Offshore Buoy	1-yr	10-yr	50-yr	100-yr
Byron Bay	5.3 (± 0.1)	7.3 (± 0.4)	8.7 (± 0.7)	9.3 (± 0.9)
Coffs Harbour	5.3 (± 0.1)	7.2 (± 0.7)	8.7 (± 1.2)	9.3 (± 1.4)
Crowdy Head ¹	5.5 (± 0.1)	6.9 (± 0.3)	7.8 (± 0.6)	8.2 (± 0.8)
Sydney	6.0 (± 0.1)	8.1 (± 0.6)	9.5 (± 1.0)	10.2 (± 1.2)
Port Kembla	5.6 (± 0.2)	7.6 (± 1.0)	8.9 (± 1.8)	9.5 (± 2.1)
Batemans Bay	5.3 (± 0.1) ²	7.3 (± 0.5)	8.9 (± 0.9)	9.6 (± 1.2)
Eden	5.8 (± 0.2)	7.9 (± 0.8)	9.4 (± 1.4)	10.1 (± 1.6)

1. The agreement in the EVA results at Crowdy Head presented in this report for concurrent hindcast and measured data was not as good as at other sites. Whilst Baird (2024) shows good time series and statistical agreement between measured and hindcast wave conditions at Crowdy Head, the EVA results presented in Section 3.1 indicates that the hindcast concurrent with the buoy dataset may be biased lower for extreme wave height compared to the measured data.
2. 1-year ARI value adopted from analysis of measured wave data set.

Table of Contents

1. Introduction	1
1.1 Overview	1
1.2 Study Motivation and Scope	1
1.3 Report Outline	2
2. Methodology.....	3
2.1 Data Sources	3
2.1.1 Offshore Wave Buoys	3
2.1.2 Wave Datasets	6
2.2 Wave Data Processing	7
2.2.1 Storm Definition	7
2.2.2 Wave Height	7
2.2.3 Wave Direction	7
2.3 Extreme Value Analysis	8
2.3.1 Probability Density Functions	9
2.3.2 Confidence Interval	9
3. Results	10
3.1 Omnidirectional Wave Height	10
3.2 Directional Wave Height	15
4. Discussion.....	17
4.1 Summary	17
4.2 Comparisons to Other Studies of Extreme Offshore Wave Height	17
4.2.1 Comparisons to Measured Data Sets	18
4.2.2 Comparison to other NSW Hindcast Data Sets	20
4.3 Recommendations for Further Studies	20
5. Acknowledgements.....	22
6. References.....	23

Appendix A	Storm Peaks Summary
Appendix B	Extreme Wave Height Analysis Results
Appendix C	Extreme Value Distributions and Parameter Estimation Methods (Taylor, 2006)
Appendix D	Extreme Wave Height Analysis Thresholds and Fit Parameters

Tables

Table E.1: Summary of extreme 1-hour exceedance omnidirectional wave height for selected ARI's based on 67-year Baird (2024) hindcast. (Values in brackets denote the 95% confidence intervals.).....	iii
Table 2.1: Summary of available wave datasets.....	3
Table 2.2: NSW Offshore Wave Buoy Locations.....	4
Table 2.3: Wave Buoy Data Availability and Effective Record Length.....	6
Table 2.4: Definition of Directional Sectors.....	8
Table 3.1: Omnidirectional Extreme Wave Height, Dataset Comparison – Sydney.....	10
Table 3.2: Omnidirectional Extreme Wave Height, Dataset Comparison – All Locations.....	12
Table 3.3: Directional EVA Comparison, Hindcast – Sydney.....	15
Table 3.4: Directional Extreme Wave Height Dataset Comparison, 20yr ARI – All Locations.....	16
Table 4.1: Summary of 1-yr, 10-yr, 50-yr and 100-yr ARI Omnidirectional wave height comparisons from measured and hindcast data sets.....	19

Figures

Figure 2.1: Locations of for NSW offshore wave buoys (2024 Deployment Locations).....	5
Figure 3.1: Omnidirectional Extreme Wave Heights Dataset Comparison – All Locations.....	13
Figure 3.2: Hindcast (1957-2023) Omnidirectional Extreme Wave Heights – All Locations.....	14

Acronyms and Abbreviations

AHD	Australian Height Datum
CM Act	NSW <i>Coastal Management Act 2016</i>
DCCEEW	NSW Department of Climate Change, Energy, Environment and Water
DPE	Former NSW Department of Planning and Environment
GEV	Generalised Extreme Value probability distribution function
H_{m0}	Frequency domain significant wave height
H_s	Time domain significant wave height
MHL	Manly Hydraulics Laboratory
MSL	Mean Sea Level
NSW	New South Wales
OEH	Former NSW Office of Environment and Heritage
POT	Peaks Over Threshold
WRB	Waverider Buoy
WRL	Water Research Laboratory

Glossary

Australian Height Datum (AHD)	A common national surface level datum approximately corresponding to mean sea level.
Average recurrence interval (ARI)	The average time between which a threshold is reached or exceeded (e.g. large wave height or high-water level) of a given value. Also known as Return Period.
Climate change	A process that occurs naturally in response to long-term variables, but often used to describe a change of climate that is directly attributable to human activity that alters the global atmosphere, increasing change beyond natural variability and trends.
Coast	A strip of land of variable width that extends from the shoreline inland to the first significant landform that is not influenced by coastal processes (such as waves, tides and associated currents).

Coastal hazard	Coastal hazards, as defined by the CM Act, include beach erosion, shoreline recession, coastal lake or watercourse entrance instability, coastal inundation, coastal cliff or slope instability, tidal inundation, and erosion and inundation of foreshores caused by tidal waters and the action of waves, including the interaction of those waters with catchment floodwaters.
Coastal processes	Coastal processes are the set of mechanisms that operate at the land-water interface. These processes incorporate sediment transport and are governed by factors such as tide, wave, and wind energy.
Directional (wave data)	Refers to wave data from a specific wave direction based on the direction of the peak spectral energy (Θ_p). Details on the directional wave sectors analysed in this study are presented in Section 2.2.3.
Extreme Storm Event	Storm for which characteristics (wave height, period, water level etc.) were derived by statistical 'extreme value' analysis. Typically, these are storms with average recurrence intervals (ARI) ranging from one to 100 years.
Geographical information system (GIS)	A system of software and procedures designed to support the management, manipulation, analysis, and display of spatially referenced data.
Extreme Value Analysis (EVA)	A statistical method to estimate the extreme exceedance probability of a particular variable using statistical distributions that are appropriate for estimating the probability of extrema events. Section 2.3 summarises the EVA methods adopted in this study.
High Tide	The maximum height reached by a rising tide. The high water is due to the periodic tidal forces and the effects of meteorological, hydrologic, and/or oceanographic conditions.
Hindcast	A dataset generated using numerical modelling of historical global atmospheric reanalysis data rather than direct <i>in situ</i> measurements.
Mean Sea Level (MSL)	MSL is a measure of the average height of the sea or ocean's surface such as the halfway point between the mean high tide and the mean low tide. At present, mean sea level is approximately equivalent to 0 mAHD (reported as 0.03 mAHD in MHL, 2019).
Nearshore	The coastal region where the sea bed influences the propagation of ocean waves. For the NSW coast this zone is generally defined as the area between the surf (breaking wave) zone and the 60m depth contour.
Omnidirectional	Refers to all wave data points in a particular data set regardless of the wave direction. Details on wave direction sectors are provided in Section 2.2.3.
Peaks Over Threshold (POT)	A data censoring procedure to filter out lower magnitude, frequently occur data values before completing an EVA. The POT approach adopted in this study is summarised in Section 2.3.
Probability	A statistical measure of the expected frequency or occurrence of particular wave conditions.

Risk	The chance of something happening that will have an impact on objectives, usually measured in terms of a combination of the consequences of an event and likelihood of occurrence.
Sea level rise	A rise in the level of the sea surface that has occurred or is projected to occur in the future, as measured from a point in time. The rise can be reported as a global mean or as measured at a specific point or estimated for a specific part of the sea or ocean.
Storm event	Any period of elevated wave height conditions. See Section 2.2 for the approach used to define storms in this report.
Storm surge	The increase in coastal water level caused by the effects of storms. Storm surge consists of two components – the increase in water level caused by the reduction in barometric pressure and the increase in water level caused by the action of wind blowing over the sea surface (wind set-up).
Storm tide	An abnormally high-water level that occurs when a storm surge combines with a high astronomical tide. The storm tide must be accurately predicted to determine the extent of coastal inundation.
Wave direction	The direction from which waves travel. The peak wave direction is the direction of waves associated with the peak period of the energy spectrum.
Wave height	The vertical distance between a wave crest and wave trough. The time-domain significant wave height, H_s , is the average of the highest one-third of waves in a measurement record. The frequency domain significant wave height, H_{m0} , is defined in Section 2.2.2.
Wave run-up	The vertical distance above mean water level reached by the uprush of water from waves across a beach or up a structure.
Wave set-up	The rise in the water level above the still water level when a wave reaches the coast. It can be very important during storm events as it results in further increases in water level above the tide and surge levels.
Waverider buoy	A buoy used to measure waves. In this report, this term refers to the range of buoys manufactured by Datawell BV.
Wind waves	Waves resulting from the action of the wind on the surface of the water.

*Many of the glossary terms here are derived or adapted from the *Coastal Management Glossary* (OEH, 2018d).

1. Introduction

1.1 Overview

The New South Wales Department of Climate Change, Energy, the Environment and Water (DCCEEW) commissioned Baird Australia Pty Ltd (Baird) to develop an update to the NSW Nearshore Wave Tool. The modelling and data framework developed during this project, comprising a web-based tool containing deepwater hindcast, transformation algorithms, model validation, and public access to nearshore wave data, provides NSW with a longstanding process for continuous improvement towards representation of nearshore wave climate for both near real-time and long-term design statistics.

This report presents an analysis of the deepwater extreme wave (height) climate at the seven (7) deepwater wave buoy locations that form DCCEEW's long term wave monitoring program that stretches along the entire length of the NSW coastline from Byron Bay in the north, to Eden in the south. Extreme value statistics, presented as Average Recurrence Interval (ARI), have been prepared based on the long term non-directional and directional wave measurement data for NSW (see Section 2.1.1) and the newly generated 67-year hindcast data set covering the period of 1957 to 2023 that has been generated for the NSW Nearshore Wave Tool (see Baird, 2024).

The scope of this study was to complete Extreme Value Analysis (EVA) on the 67-year hindcast data presented in Baird (2024) for the offshore NSW buoy locations, and to compare estimates of extreme wave heights from the 67-year hindcast, with estimates derived from EVA of the measured buoy data. Details of the report structure are presented in Section 1.3.

It is important to note that this report is not intended to replace or update the detailed storm type and storm climatology description presented in Shand *et al* (2011) and this study does not present a detailed critique of the extreme wave climate from other studies including Shand *et al* (2011) and Glatz *et al* (2017), compared to those presented in this report. However, this report discusses in Section 2.3 the EVA methods adopted in this study and how they differ from both those studies. A brief summary comparison of extreme wave climate results from Shand *et al* (2011) and Glatz *et al* (2017) for the buoy locations presented in this report is included in Section 4.2.

1.2 Study Motivation and Scope

A detailed understanding of the spatial and temporal variability in oceanic and nearshore wave climates is essential to better assess the present and future risks of coastal hazards, such as erosion and inundation (e.g. Kinsela *et al.*, 2017; Hanslow *et al.*, 2017; Morris *et al.*, 2016). Previously, DCCEEW (then the Office of Environment and Heritage, OEH) developed an NSW Coastal Ocean Wave Model System, comprising coupled WAVEWATCH-III (WW3) and SWAN spectral wave models. The system was used to develop a 35-year wave hindcast using Climate Forecast System Reanalysis (CFSR) wind forcing (Cardno 2012; Kinsela *et al.* 2014), and a 60-year wave hindcast (1950-2009) using down-scaled reanalysis wind fields generated by the NSW/ACT Regional Climate Modelling (NARClIM v1.0) project (Dent *et al.* 2014). The 35-year CFSR hindcast (Cardno 2012; Kinsela *et al.* 2014) had reasonable model validation but did not include wave data prior to 1979 and was underbias in its representation of the longer return period wave conditions and had relatively high uncertainty in directional extreme wave climate estimates. Overall, the 60-year wave NARClIM 1.0 hindcast (1950-2009) reported in Dent *et al* (2014) did not have good agreement with the measured wave climate compared to the CFSR hindcast and the available NSW coastal wave measurements available at that time.

In 2016, OEH engaged Baird to develop the NSW Nearshore Wave Transformation Toolbox that included a statewide nearshore wave transformation tool capable of providing long-term nearshore wave hindcasts

and design nearshore wave conditions. Since the development of the NSW Nearshore Wave Transformation Toolbox in 2017 (Baird, 2017), the State Government has collected fundamental coastal datasets including high-resolution bathymetry covering the entire coastline and measured nearshore wave buoy data at 18 locations (see Kinsela et al., 2024).

The new data provided the opportunity to update and improve the tools by incorporating high-resolution seabed data in the underlying wave model and rigorously calibrating and evaluating nearshore wave predictions in NSW coastal settings. In addition, a key aim of the Toolbox update was to make the tools readily available to external research and management stakeholders in an all new online coastal wave modelling application. A key component in developing the updated NSW Nearshore Wave Tool was the development of a long duration deepwater hindcast of spectral wave data along the NSW coast. The deepwater spectral hindcast covers the period 1957 to 2023 using ERA5 wind-forcing WW3 wave model system as reported in Baird (2024). The development and validation of the updated NSW Nearshore Wave Tool including the development of the deepwater hindcast is described in Baird (2024).

The NSW Nearshore Wave Tool deepwater hindcast presents the opportunity to prepare an updated analysis of the extreme wave climate of the NSW coast. Previous studies such as Shand *et al* (2011) and Glatz *et al* (2017) have conducted extreme value analysis (EVA) of data collected by the seven deepwater wave buoys maintained by Manly Hydraulics Laboratory (MHL) for DCCEE. This study updates the EVA conducted on the measured wave buoy data and extends the analysis to the deepwater hindcast prepared for the NSW Nearshore Wave Tool. The hindcast covers the period 1957 to 2023 inclusive and so allows an assessment of the extreme wave climate of the NSW coast which includes the large storms experienced during the 1970's. This information is critical to better understanding and modelling how coastal hazards will impact the NSW coast, especially with a changing climate, see for example Shand *et al* (2010)).

1.3 Report Outline

This report is structured into the following sections:

- Section 2: Study methodology including:
 - Section 2.1: Description and references of data sets applied in this study;
 - Section 2.2: Description of wave data POT censoring methods; and
 - Section 2.3: Summary of Extreme Value Analysis (EVA) methods adopted in this study.
- Section 3: Results from the EVA including:
 - Section 3.1: Omnidirectional wave height;
 - Section 3.2: Directional wave height for three directional sectors (defined in Section 2.2.3).
- Discussion of results including:
 - Section 4.1: Summary of omnidirectional and directional deepwater wave height along the NSW coast;
 - Section 4.2: Comparison of deepwater omni-directional wave heights to earlier studies; and
 - Section 4.3: Recommendations for further studies and analyses.

2. Methodology

The overall approach and methods have been adopted from the methods used for the analysis presented in Shand *et al* (2011) with some adjustments which will be discussed in this section.

2.1 Data Sources

The data sources adopted in this study are summarised in Table 2.1.

Table 2.1: Summary of available wave datasets.

Source	Description	Temporal Resolution
NSW Deepwater Wave Buoys	The MHL wave buoy program commenced in 1974 at one location and expanded to seven locations by 1986. Wave buoy deployments at these seven locations have been ongoing to the present, providing a valuable long-term dataset, with coverage along the NSW coast. The locations and available data periods are summarised in Section 2.1.1.	Early records provide 3-hourly and 6-hourly measurements, with all sites providing 1-hourly records from 1984 and 1985. Only the 1-hourly records have been used for this study.
ERA5	Synoptic wind fields were obtained from the ERA5 long duration global hindcast reanalysis model (Hersbach <i>et al</i> , 2020) for use in the development of the wave hindcast. ERA5 is the fifth generation hindcast from the European Centre for Medium-Range Weather Forecasts (ECMWF) and provides hourly estimates for many atmospheric, ocean-wave and land-surface quantities on a regular geographic (latitude-longitude) grid of 0.125° (\approx 12-13 km) horizontal resolution.	1-hourly
Deepwater Wave Hindcast	The hindcast is made up of a WW3 wave model system, using the ERA5 global wind forcing from 1957 to 2023 inclusive. The model development and validation are described in Baird (2024). Wave spectra time-series have been generated for each of the seven MHL WRB locations with summary wave parameters calculated for use in this analysis.	1-hourly

2.1.1 Offshore Wave Buoys

The NSW wave buoy program commenced in February 1974 with the deployment of a wave buoy at Port Kembla. This program was progressively expanded to seven locations as summarised in Table 2.2 (and illustrated in Figure 2.1) with the seventh wave buoy location deployed at Batemans Bay in May 1986. All locations initially used non-directional wave buoys, with the first directional wave buoy deployed at Sydney in 1992. Since 2012, all locations collect directional wave measurements. The NSW wave buoy program is managed by MHL with funding from DCCEEW.

The wave buoy deployment locations have changed over the course of the program, with the full deployment location history available in MHL (2022). Table 2.2 provides the present deployment location of the wave buoys with the offshore locations indicated in Figure 2.1. This analysis does not make allowance for these changes in deployment location and the analysis is made on the assumption that the wave buoy data is representative of a single location at each site. The most notable deployment location and depth changes occurred during the earliest years of the NSW wave buoy program prior to 1980, and these records are not included in the analyses presented in this report due to the less frequent data capture intervals for those earlier records. The Byron Bay deployment location has experienced the largest changes of the included measured data, with the location shifting approximately 25 km south from offshore Cape Byron to offshore Ballina. The deployment depth and the bathymetric gradients for incident wave energy have remained reasonably consistent between the two deployment locations. Similarly, the Eden deployment location has experienced changes within an approximately 20 km range with associated deployment depths ranging between 80 and 100 metres. The wave exposure at these locations are considered to be similar based on the known bathymetry in this region.

Table 2.2: NSW Offshore Wave Buoy Locations.

Location	First Deployment Date	2024 Deployment Location	2024 Water Depth (m)
Byron Bay	14/10/1976	28 52'14" 153 41'39"	62
Coffs Harbour	26/05/1976	30 16'40" 153 16'40"	72
Crowdy Head	11/10/1985	31 49'01" 152 51'03"	79
Sydney	17/07/1987	33 46'26" 151 24'42"	90
Port Kembla	7/02/1974	34 28'35" 151 01'33"	80
Batemans Bay	27/05/1986	35 44'25" 150 19'03"	65
Eden	8/02/1978	37 15'57" 150 11'36"	100



Figure 2.1: Locations of for NSW offshore wave buoys (2024 Deployment Locations).

The wave buoy program captured data at 12 or 6-hour intervals until 1984 when the first location was upgraded to capture data at 1-hour intervals. All locations were collecting data at 1-hour intervals by 1985 (and Sydney from this location's first deployment in 1987). For consistency, this analysis only utilises the available 1-hour interval records from each location. The available data periods are summarised in Table 2.3. The effective record length is presented which accounts for all available data excluding outages and data flagged as bad by MHL quality control processes.

Table 2.3: Wave Buoy Data Availability and Effective Record Length.

Location	Start Date		End Date	Effective Record Length (years)	
	Hourly	Directional		Hourly	Directional
Byron Bay	28/06/1984	26/10/1999	31/12/2023	32.7	20.4
Coffs Harbour	27/06/1984	14/02/2012	31/12/2023	34.4	10.4
Crowdy Head	10/10/1985	19/08/2011	31/12/2023	33.6	11.1
Sydney	17/07/1987	3/03/1992	31/12/2023	33.7	29.3
Port Kembla	14/06/1984	20/06/2012	31/12/2023	34.2	9.3
Batemans Bay	27/05/1986	23/02/2001	31/12/2023	33.9	20.3
Eden	27/03/1985	16/12/2011	31/12/2023	34.3	10.4

2.1.2 Wave Datasets

Three datasets have been prepared for each of the wave buoy locations as described below:

- **Measured:** This dataset consists of all available hourly records from each of the wave buoy locations. The available data periods are described in Table 2.3.
- **Hindcast Concurrent:** This dataset consists of all hindcast data for each wave buoy location during the available date range for the Measured dataset. Gaps in the measured dataset have not been reproduced, so this dataset consists of a continuous 1-hourly record for the full measured data period as described in Table 2.3.
- **Hindcast:** This dataset consists of all 1-hour continuous hindcast data for the period 67-year period between 1957 to 2023 (inclusive) for each wave buoy location.

The EVA analysis has been prepared for each of these datasets to provide comparison of the results. Given that the measured wave data for most locations commences with non-directional measurements prior to directional wave buoys being deployed, there is a further distinction in datasets between the available non-directional and directional measurement periods for each location. The Hindcast Concurrent datasets match these available measured data periods for the relevant analyses of omnidirectional and directional sector cases.

2.2 Wave Data Processing

2.2.1 Storm Definition

A 3.0 metre H_{m0} threshold has been adopted as the POT value to prepare the initial storm peak datasets for this study, with this threshold applied to all 1-hourly records. A 3.0 m threshold has been selected for previous studies on the NSW wave climate (Harley *et al* 2010) and for global studies on changes to coastal wave storminess (Lobeto *et al*, 2024). A minimum interval between storms of 24 hours was adopted to ensure that each storm was independent, and to limit the number of short-duration events in a manner consistent with Shand *et al* (2011). Longer duration storm thresholds have not been analysed in this study. For all cases, higher wave height thresholds have been adopted to ensure best fit to the probability distribution functions as described further in Section 2.3.1.

The storm definition adopted for this analysis largely follows the Peaks Over Threshold (POT) approach described in Shand *et al* (2011). The POT approach remains the preferred method, as recommended in Goda (2000), over both the alternative annual maxima and total sample methods. The annual maxima method results in a relatively small storm sample size with associated larger confidence intervals, while the total sample method does not meet the assumption of sample independency due to the long duration of storm wave events observed along the NSW coast. In this study, a higher wave height threshold has been adopted compared to Shand *et al* (2011) and Glatz *et al* (2017) which both adopted a POT of 3.0 m for storm events up to 24-hours duration. A higher wave height threshold than adopted in those studies is now possible with the longer duration measured and hindcast data sets available in this study, and as discussed in Section 2.3, the lower wave height thresholds adopted in those earlier studies are not always appropriate extreme value analysis as too many samples may be too small and frequent in occurrence to be classified as extreme events based on the definition specified in Goda (2000).

2.2.2 Wave Height

The wave height parameter used in this analysis is the frequency domain significant wave height, H_{m0} , defined in Equation 2.1. This parameter differs to the parameter used in previous EVA analyses where the time domain significant wave height, H_s has been used. H_s is the average of the highest one-third of waves in a measurement period using the zero up-crossing wave definition. The long duration deepwater wave hindcast has been developed using a spectral wave model, providing frequency domain wave parameters. As a result, H_{m0} is preferred to H_s .

$$H_{m0} = 4\sqrt{m_0} \quad (\text{Eq. 2.1})$$

The available MHL wave buoy measurements do not consistently provide the H_{m0} or zero spectral moment, m_0 , parameters and for some earlier periods where these frequency domain parameters are available, the data appear noisy. For all measured wave buoy records, the H_{m0} has been estimated by using the time domain H_s with a scaling factor of 1.05 applied. This scaling factor is consistent with the theoretical relationship between H_s and H_{m0} in intermediate water depths based on Goda (2000), and this scaling factor has been verified in this study by review of measured data where both parameters are reported concurrently.

2.2.3 Wave Direction

The wave direction parameter adopted for this study is the direction at the peak spectral energy, Θ_p . In addition to an omnidirectional analysis, three directional sectors have been considered as described in Table 2.4 (i.e. NE, ESE and S). Each storm has been included in the relevant directional sector storm peak dataset if the peak wave direction occurs within the directional sector at any time during the full duration of the event, not only at the time of the peak wave height. That is, a single storm event can be included in multiple directional sector datasets with the peak wave height from each sector adopted respectively, using the wave height threshold selected for each directional sector. This approach differs to

the automated EVA tools available in the online The NSW Nearshore Wave Tool (see Baird, 2024) where only the peak direction at the time of the storm peak wave height is considered.

Table 2.4: Definition of Directional Sectors.

Sector	Abbreviation	Directions
Omnidirectional	Omni	All non-directional and directional data
North-east	NE	0 – 90 degrees
East-southeast	ESE	90 – 135 degrees
South	S	135 – 225 degrees

Appendix A presents summary plots of the directional storm peaks for each location and dataset. Also provided on these figures are the dates of the highest ten omnidirectional storm peaks for each dataset.

2.3 Extreme Value Analysis

Statistics for storm wave heights at the selected offshore locations using measured and hindcast wave data sets have been derived by Extreme Value Analysis (EVA) methods that have been developed from well-established references outlined in Taylor et al (2006) with the primary reference for the EVA method, being the widely adopted procedures in Goda (2000). The EVA has focused on applying best practice methods to ensure that the following principals of EVA are adhered too:

- The storm wave data sets are formed from independent, event peak wave height data points and the data samples are formed from extreme data points, not biased with data samples from wave conditions that occur frequently (i.e. modal conditions).
- Parameters for the extreme value distributions are calculated using Maximum Likelihood Estimation (MLE) as recommended by Goda (2000).
- Confidence intervals, which define the range of uncertainty in extreme wave height for a specified return period, have been calculated using bootstrapping procedure which calculates uncertainty explicitly based on each individual data set rather than applying empirical or fixed probability function assumptions.

Extreme wave height distributions for the NSW deepwater buoy locations have been prepared in recent studies including Shand *et al* (2011) and Glatz *et al* (2017). It is beyond the scope of this study to provide a detailed review of the assumptions and EVA methods adopted in those studies; however, the following were considered, when developing the EVA methods adopted within this study:

- Both Shand *et al* (2011) and Glatz *et al* (2017) adopted relatively low significant wave height thresholds of 3 m for storm durations up to 24 hours. This is a low threshold that is frequently exceeded and has the potential to bias the EVA parameters to the large population of events with wave heights between 3 and 4.5 m, rather than being formed from data sets that representative of extreme events with return periods greater than 1-year ARI.
- Shand et al (2011) considered a range of extreme value distributions to apply to the NSW data and evaluated in detail the FT-1 (Gumbel, Type-I) and Weibull (Type-III) distributions based on recommendations in You (2007). Shand *et al* (2011) ultimately adopted Weibull distribution based on improved goodness of fit statistics compared to the FT-1 distribution. Glatz et al (2017) generally adopted methods consistent with Shand *et al* (2011) and also ultimately adopted the Weibull distribution.
- Both Shand *et al* (2011) and Glatz *et al* (2017) used Goda (2000)'s empirical formulas for estimating confidence intervals which assume that the best fit estimate of the extreme value is the 'true'

distribution. Where data records are small, or heavily bias by one or two events that are exceptionally larger than other samples in the sample, this assumption is unlikely to be valid. The use of data driven methods to derive confidence intervals can provide an improved definition of uncertainty that better accounts for the sample size and spread in data values as noted in Taylor *et al* (2006).

In response to the above key points, Baird has utilised our inhouse EVA analysis methods, which are implemented in the NSW Nearshore Waves toolbox. Baird's software adopted the distribution fitting and confidence interval calculation as described in Taylor (2006) adopting the methods recommended in Goda (2000) and Coles (2001). The following sections present details of the EVA methods that Baird has adopted for the NSW wave data sets as follows:

- Section 2.3.1 outlines the Probability Density Function adopted by Baird which was the Generalised Extreme Value (GEV) distribution due to its greater flexibility in fitting to the larger values in the extreme value sample; and
- Section 2.3.2 outlines Baird's bootstrapping-based confidence interval estimation method.

2.3.1 Probability Density Functions

Baird's EVA toolbox includes the Type-I (Gumbel), Type-III (Weibull) and Generalised Extreme Value (GEV) distributions; for this study the GEV distribution was adopted. The GEV distribution provides the potential for more non-linearity in the fitted distribution. As outlined in Coles (2001), the GEV distribution can have a very heavy tail as it tends to a Type II (Frechet) distribution where the magnitude of the variable being analysed continues to increase exponentially as likelihood of occurrence reduces. This can be beneficial in terms of the ability to fit better to the largest one or two values in the sample set. However, these are potential limitations of the GEV distribution compared to Weibull distribution when the extreme sample data sets are small or not well formed. In both those scenarios, the GEV fit can become unstable. For this study, the data records (measured and hindcast) were suitably large that well-formed extreme values samples could be formed for all data sets. It is not considered necessary to provide equations of the various statistical distributions discussed in this section. 0 provides a copy of Taylor (2006) which presents equations and details on maximum likelihood parameter estimation for Type-I, Type-II and Type-III extreme value distributions that are based primarily on Goda (2001). Coles (2001) provides the details on the GEV distribution which combines Type-I, Type-II and Type-III into a single extreme value distribution and, depending on the fit to each unique data set, the GEV distribution can take the form of either a Type-I (Gumbel), Type II (Frechet) or Type-III (Weibull) distribution, or somewhere between those statistical distribution form.

In accordance with EVA theory, as presented in Goda (2000), a Peak Over Threshold (PoT) censoring approach was adopted to only fit the GEV distribution to extreme, independent storm data values in the hindcast data set above a specified POT value. In general, a threshold wave height was selected to optimise the extreme value fit, and to also ensure that the storm frequency in the data set were approximately two to three (2-3) per year for omni-directional wave height analyses, and at least one to two (1-2) per year for directional wave height analyses. The selected wave height thresholds adopted for all datasets and directional cases are presented in Appendix D.

The parameters for the all the EVA distributions evaluated by Baird were determined using a Maximum Likelihood technique as recommended by Goda (2000) and Coles (2001). For the Weibull distribution, the intercept parameter was determined by minimising the residual error, whereas for the GEV distribution all parameters were calculated using the Maximum Likelihood technique.

2.3.2 Confidence Interval

The confidence interval method adopted in this study is described in Taylor (2006) and is based on the recommended techniques for fitting data sets by van Vledder *et al* (1993), Goda (2000) and Coles (2001). For the GEV distribution, confidence intervals were determined using a boot-strapping procedure using a method adapted from that described by Naess and Hungnes (2002).

3. Results

Extreme wave height analyses have been performed for each location using the three datasets described in Section 2.1.2, and for each dataset the four directional sectors described in Section 2.2.3 have been considered (i.e. Omni; NE; ESE; S). Comparison of the fitted probability distribution function between the three datasets is presented in this section for the omnidirectional case to allow assessment of the agreement between the measured and hindcast data over the period of available measured wave data, and for the longer duration hindcast over the full 1957 to 2023 period in Section 3.1. A summary of the directional sector analyses is provided in Section 3.2. Detailed presentation of the hindcast extreme wave height analysis results are provided including figures presenting the fitted probability distribution functions to the storm peaks in Appendix B. Given that the full hindcast covers a longer period than the measured wave datasets, these hindcast results provide a higher level of confidence in longer return period extreme wave heights than possible using measured wave data alone.

Appendix B provides tables of omnidirectional and directional sector extreme wave heights by location for each of the three datasets. Figures are provided showing the plotted storm peaks and fitted EVA for the Hindcast dataset for each directional sector presented by location.

Appendix D presents the selected wave height threshold for each location and directional sector, along with the corresponding best fit shape parameters. At all sites and directional data sets, the GEV distribution is a Type III (Weibull-like) distribution.

3.1 Omnidirectional Wave Height

The agreement between the measured and hindcast datasets has been assessed by comparing the extreme wave height analysis for corresponding time periods for each location. Listed in Table 3.1 are the analysis results for each omnidirectional dataset for the Sydney buoy location and Figure 3.1 presents plots of these comparisons for all locations. Further comparison for all locations is listed in Table 3.2 for selected ARI durations. Figure 3.2 presents the plotted storm peak wave heights for the omnidirectional Hindcast dataset at each location, along with the GEV fit and associated 95% confidence intervals in grey shading. Overlap of the 95% confidence intervals is indicated by darker shading and full results are provided in Appendix B.

Table 3.1: Omnidirectional Extreme Wave Height, Dataset Comparison – Sydney.

ARI	Measured		Hindcast Concurrent		Hindcast	
	H_{m0} (m)	95% CI ($\pm m$)	H_{m0} (m)	95% CI ($\pm m$)	H_{m0} (m)	95% CI ($\pm m$)
years						
1	6.18	0.19	5.93	0.17	5.98	0.13
2	6.71	0.24	6.51	0.27	6.60	0.24
5	7.37	0.38	7.23	0.44	7.43	0.42
10	7.86	0.53	7.75	0.61	8.05	0.58
20	8.33	0.71	8.27	0.79	8.68	0.75
50	8.94	0.97	8.93	1.06	9.52	1.00
100	9.39	1.18	9.43	1.29	10.15	1.21

ARI	Measured		Hindcast Concurrent		Hindcast	
200	9.84	1.41	9.91	1.52	10.78	1.42
500	10.42	1.72	10.55	1.84	11.62	1.72



Table 3.2: Omnidirectional Extreme Wave Height, Dataset Comparison – All Locations.

	Average Recurrence Interval (years)								
	1			20			100		
<i>Dataset</i>	<i>Measured</i>	<i>Hindcast Concurrent</i>	<i>Hindcast Full</i>	<i>Measured</i>	<i>Hindcast Concurrent</i>	<i>Hindcast Full</i>	<i>Measured</i>	<i>Hindcast Concurrent</i>	<i>Hindcast Full</i>
Location	H_{m0} (m) \pm 95% CI (m)			H_{m0} (m) \pm 95% CI (m)			H_{m0} (m) \pm 95% CI (m)		
Byron Bay	5.46 \pm 0.18	5.19 \pm 0.11	5.27 \pm 0.09	7.17 \pm 1.16	7.55 \pm 0.81	7.87 \pm 0.53	8.11 \pm 1.86	8.87 \pm 1.31	9.31 \pm 0.85
Coffs Harbour	5.63 \pm 0.16	5.28 \pm 0.10	5.27 \pm 0.14	7.52 \pm 0.57	7.46 \pm 1.90	7.83 \pm 0.89	8.43 \pm 0.92	8.63 \pm 3.21	9.27 \pm 1.40
Crowdy Head	5.62 \pm 0.12	5.34 \pm 0.06	5.45 \pm 0.07	7.59 \pm 0.65	7.23 \pm 0.54	7.34 \pm 0.44	8.66 \pm 1.19	8.11 \pm 0.97	8.21 \pm 0.75
Sydney	6.18 \pm 0.19	5.93 \pm 0.17	5.98 \pm 0.13	8.33 \pm 0.71	8.27 \pm 0.79	8.68 \pm 0.75	9.39 \pm 1.18	9.43 \pm 1.29	10.15 \pm 1.21
Port Kembla	5.78 \pm 0.16	5.59 \pm 0.04	5.62 \pm 0.20	8.04 \pm 0.81	7.66 \pm 0.67	8.13 \pm 1.34	9.27 \pm 1.29	8.80 \pm 1.12	9.50 \pm 2.11
Batemans Bay	5.29 \pm 0.05	-	-	7.29 \pm 0.73	7.36 \pm 0.79	8.00 \pm 0.64	8.39 \pm 1.29	8.59 \pm 1.35	9.56 \pm 1.15
Eden	5.93 \pm 0.22	5.78 \pm 0.22	5.80 \pm 0.18	8.40 \pm 0.97	8.08 \pm 0.89	8.57 \pm 1.06	9.72 \pm 1.48	9.28 \pm 1.37	10.07 \pm 1.64

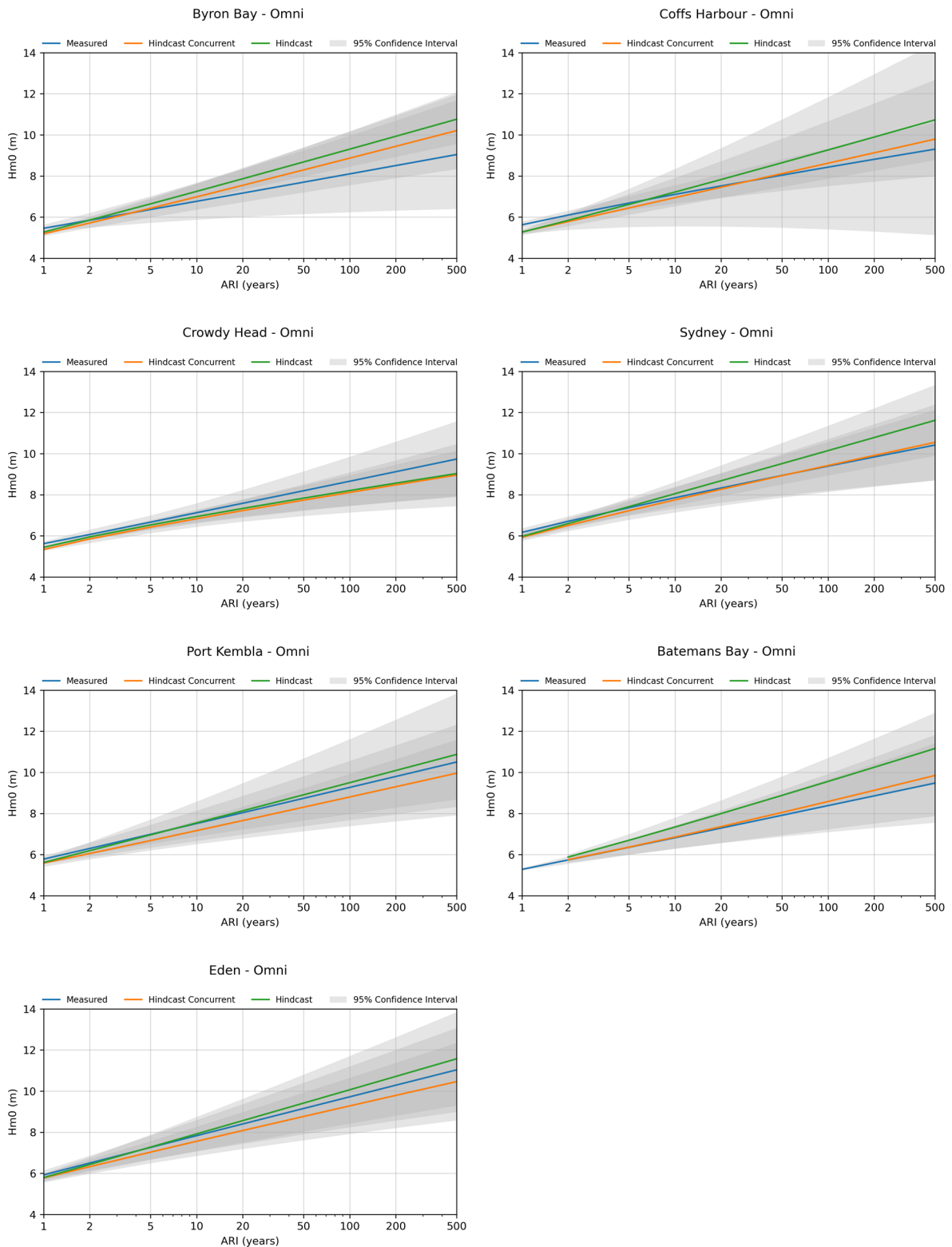


Figure 3.1: Omnidirectional Extreme Wave Heights Dataset Comparison – All Locations.



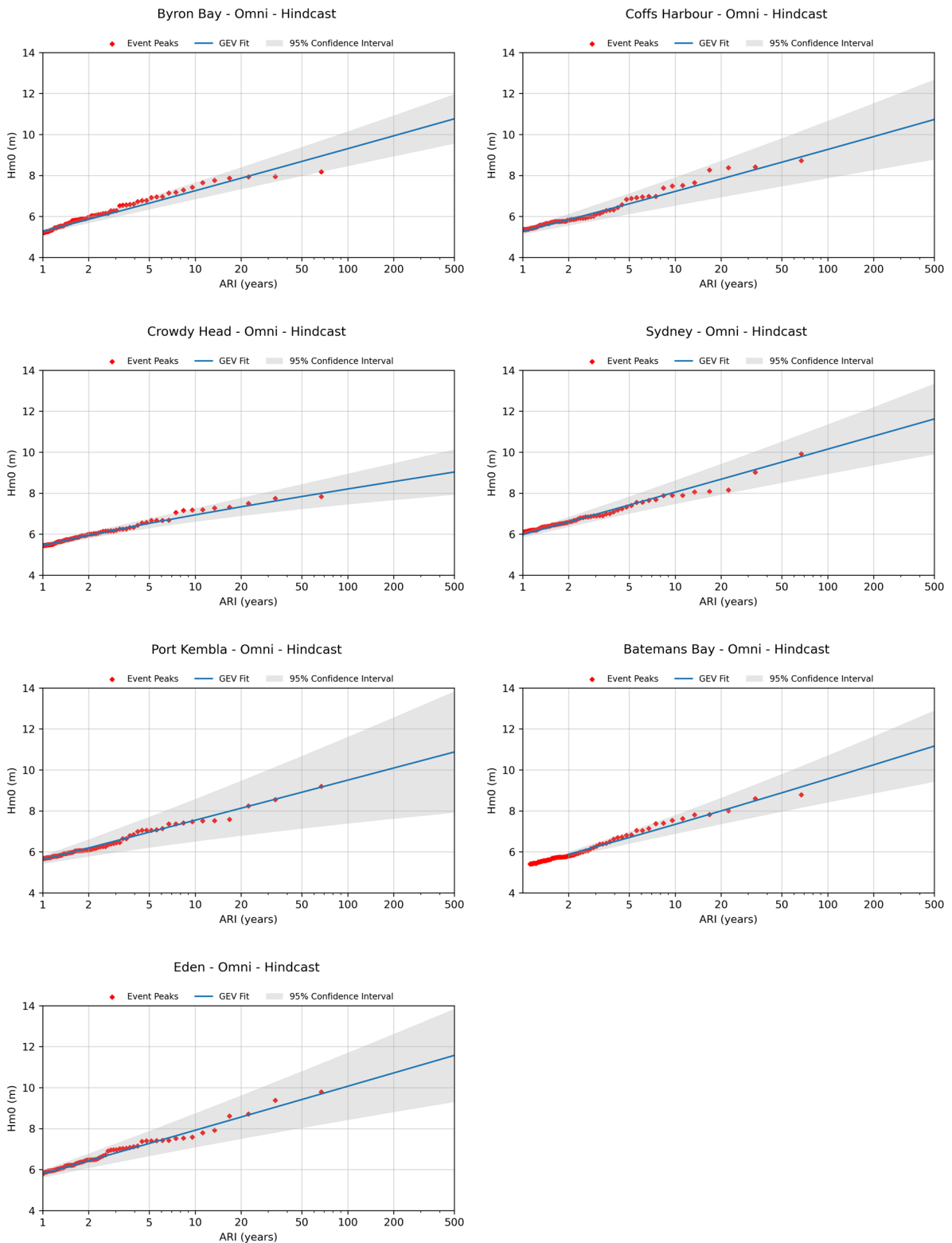


Figure 3.2: Hindcast (1957-2023) Omnidirectional Extreme Wave Heights – All Locations.



3.2 Directional Wave Height

A directional extreme value analysis was carried out for all buoy locations, retaining the directional sectors adopted in Shand (2010). Listed in Table 3.3 are the analysis results of each directional sector for the Sydney Hindcast dataset. Comparison of directional results for all locations and datasets for the 20-year ARI are listed in Table 3.4.

It is noted that 4 of the 7 buoys (except for Byron Bay, Sydney and Batemans Bay) have short duration measured data sets of less than 11 years measured directional wave data, and as a result have a relatively low number of recorded storm events, particularly for the NE and ESE directional sectors. While the GEV distribution applied in this study performed very well for the omni-directional analysis, with an improved description of the non-linearity of larger storms, this was more challenging for the directional analyses due to the low number of storm events, including for the extended 67-year hindcast. As such, the directional criteria presented in this report should be considered with caution.

Table 3.3: Directional EVA Comparison, Hindcast – Sydney

ARI	Omni	NE	ESE	S
years	All directions	0° - 90°	90° - 135°	135° - 225°
H_{m0} (m) \pm 95% CI (m)				
1	5.98 \pm 0.13	3.51 \pm 0.04	-	5.79 \pm 0.13
2	6.60 \pm 0.24	4.09 \pm 0.17	5.75 \pm 0.06	6.39 \pm 0.28
5	7.43 \pm 0.42	4.87 \pm 0.30	6.54 \pm 0.33	7.16 \pm 0.54
10	8.05 \pm 0.58	5.46 \pm 0.42	7.18 \pm 0.56	7.73 \pm 0.77
20	8.68 \pm 0.75	6.05 \pm 0.57	7.84 \pm 0.83	8.29 \pm 1.03
50	9.52 \pm 1.00	6.84 \pm 0.78	8.73 \pm 1.22	9.02 \pm 1.41
100	10.15 \pm 1.21	7.43 \pm 0.96	9.41 \pm 1.54	9.57 \pm 1.71
200	10.78 \pm 1.42	8.03 \pm 1.15	10.11 \pm 1.88	10.11 \pm 2.03
500	11.62 \pm 1.72	8.82 \pm 1.42	11.03 \pm 2.35	10.83 \pm 2.46

Table 3.4: Directional Extreme Wave Height Dataset Comparison, 20yr ARI – All Locations.

Directional Sector	NE 0° - 90°			ESE 90° - 135°			S 135° - 225°		
Dataset	Measured	Hindcast Concurrent	Hindcast Full	Measured	Hindcast Concurrent	Hindcast Full	Measured	Hindcast Concurrent	Hindcast Full
Location	H _{m0} (m) ±95% CI (m)								
Byron Bay	6.63 ±1.74	7.43 ±1.31	7.67 ±0.57	7.35 ±2.06	6.44 ±1.31	7.20 ±0.94	6.94 ±0.79	6.69 ±0.53	6.74 ±0.89
Coffs Harbour	7.77 ±1.78	7.39 ±1.53	7.34 ±0.78	6.56 ±1.02	6.60 ±3.41	7.77 ±0.77	7.64 ±1.08	7.72 ±1.15	7.41 ±0.66
Crowdy Head	6.96 ±2.06	7.17 ±1.45	6.71 ±0.78	6.57 ±1.41	6.02 ±2.23	6.57 ±0.50	6.54 ±0.70	7.28 ±1.10	7.16 ±0.46
Sydney	6.24 ±0.66	6.16 ±0.95	6.19 ±0.57	7.61 ±0.96	7.60 ±0.97	7.84 ±0.83	8.47 ±0.80	8.36 ±0.93	8.29 ±1.03
Port Kembla	6.29 ±1.37	6.33 ±1.79	6.22 ±0.61	6.72 ±1.27	6.81 ±2.00	7.09 ±1.20	7.83 ±1.27	7.61 ±1.04	7.68 ±1.35
Batemans Bay	6.40 ±1.49	6.58 ±1.62	7.13 ±0.81	7.01 ±0.97	6.90 ±0.71	7.80 ±0.83	7.33 ±0.71	7.24 ±0.69	7.25 ±0.80
Eden	9.24 ±3.70	8.63 ±1.48	7.90 ±0.93	7.65 ±1.54	7.31 ±1.34	8.27 ±0.90	8.68 ±1.88	7.97 ±1.38	8.30 ±0.91

4. Discussion

4.1 Summary

The EVA results presented in Section 3 provide new insights into the extreme NSW offshore wave climate compared to earlier studies including Shand *et al* (2011), Cardno (2012), and Glatz *et al* (2017). With the exception of Crowdy Head, at all other offshore wave buoy locations the EVA of the 67-year continuous hindcast data set reported in Baird (2024) has resulted in an increase in the estimates of the extreme wave heights for 50-years ARI and greater compared to using the hindcast data set only during the period of concurrent coastal wave buoy measurements. At Crowdy Head, the 67-year hindcast generally has slightly lower wave heights (≈ 0.2 m Hs) for extreme value return period compared to those other studies.

The 67-year hindcast data set has also improved the estimates of extreme directional wave climate, particularly for characterising the frequency of larger storms with waves from the northeast to east offshore wave direction that occur less frequently than large southeast to south offshore waves, particularly south of Coffs Harbour.

The EVA method adopted in this analysis is documented in Section 2.3. Section 4.2 presents comparisons of the extreme wave climate results from this study, with those presented in Shand *et al* (2011) and Glatz *et al* (2017). Two key differences in the EVA methods adopted in this analysis compared to Shand *et al* (2011) and Glatz *et al* (2017) are:

- This study has set higher wave height thresholds to form extreme value data sets compared to both those studies. As a result, the EVA results presented in this study are generally fitted to data sets that have an average storm frequency of 2 to 3 events per year for omnidirectional data sets, and 1 to 2 events per year for directional data sets. Shand *et al* (2011) and Glatz *et al* (2017) both adopted a wave height threshold of 3 m for the EVA presented those studies. The higher threshold selected in this study, which is assisted by the longer duration of the measured and hindcast data sets available in study, is more aligned with the recommendations in Goda (2000) regarding the selection of data sets that are representative of extreme storms, rather than conditions that are exceeded on many occasions each year. Refer to 0 for the selected thresholds for each data set and directional case.
- This study has also adopted the GEV distribution, rather than the Weibull distribution that was favoured in Shand *et al* (2011) and Glatz *et al* (2017). The GEV distribution provides the potential for increased non-linearity in the fitted extreme value distribution and in this study the GEV distribution has generally increased the 100-year ARI wave height estimates. The fitting of the GEV distribution, compared to Weibull (Type-III) and Gumble (Type-I), is more sensitive to the relative magnitude characteristics of particular data sets, but since the GEV distribution combines three potential extreme value distributions (Type-I, Type-II and Type-III) it provides a quantitative and objective approach to tailor an extreme value fit to the characteristics of each site and particular data set.

4.2 Comparisons to Other Studies of Extreme Offshore Wave Height

The following sections provide a summary of comparisons of the omnidirectional extreme wave climate using measured and the 67-year hindcast presented in this report, with those presented in Shand *et al* (2011) and Glatz *et al* (2017) based on the measured data sets available at the time of those studies. It should be noted that this study adopted different EVA methods, as summarised in Section 4.1, as well as having access to longer duration measured and hindcast offshore wave data sets.

4.2.1 Comparisons to Measured Data Sets

Table 4.1 presents a summary of the EVA results from (2011) and Glatz *et al* (2017) based on measured buoy data available at the time of those studies, with the measured data available for this study and the 67-

year hindcast data set presented in Baird (2024). Overall, the EVA comparisons between the three measured data sets are comparable up to 10-years ARI, with the Baird and Glatz *et al* (2017) EVA results having high estimates for 50- and 100-year ARI wave heights, particularly at Sydney and Eden. The 67-year hindcast data set, with the exception of Crowdy Head, has higher estimates of 10 to 100-years ARI wave heights than the analyses on measured data.



Table 4.1: Summary of 1-yr, 10-yr, 50-yr and 100-yr ARI Omnidirectional wave height comparisons from measured and hindcast data sets.

Offshore Buoy Location	1yr ARI - Omnidirectional				10yr ARI - Omnidirectional				50yr ARI - Omnidirectional				100yr ARI - Omnidirectional			
	Shand ¹	Glatz ²	Baird ³	Baird 67yr ⁴	Shand ¹	Glatz ²	Baird ³	Baird 67yr ⁴	Shand ¹	Glatz ²	Baird ³	Baird 67yr ⁴	Shand ¹	Glatz ²	Baird ³	Baird 67yr ⁴
Byron Bay	5.2 (0.2)	5.3 (0.2)	5.5 (0.2)	5.3 (0.1)	6.4 (0.2)	6.6 (0.2)	6.8 (0.9)	7.3 (0.4)	7.2 (0.3)	7.5 (0.3)	7.7 (1.6)	8.7 (0.7)	7.6 (0.3)	7.8 (0.3)	8.1 (1.9)	9.3 (0.9)
Coffs Harbour	5.2 (0.2)	5.3 (0.2)	5.6 (0.2)	5.3 (0.1)	6.7 (0.3)	7.0 (0.3)	7.1 (0.4)	7.2 (0.7)	7.7 (0.4)	8.1 (0.4)	8.0 (0.8)	8.7 (1.2)	8.1 (0.4)	8.6 (0.5)	8.4 (0.9)	9.3 (1.4)
Crowdy Head	5.4 (0.2)	5.4 (0.2)	5.6 (0.1)	5.5 (0.1)	7.0 (0.4)	7.0 (0.3)	7.1 (0.5)	6.9 (0.3)	8.0 (0.5)	8.0 (0.4)	8.2 (0.9)	7.8 (0.6)	8.5 (0.5)	8.4 (0.5)	8.7 (1.2)	8.2 (0.8)
Sydney	5.9 (0.2)	5.8 (0.2)	6.2 (0.2)	6.0 (0.1)	7.5 (0.4)	7.6 (0.3)	7.9 (0.5)	8.1 (0.6)	8.6 (0.5)	8.9 (0.4)	8.9 (1.0)	9.5 (1.0)	9.0 (0.5)	9.4 (0.5)	9.4 (1.2)	10.2 (1.2)
Port Kembla	5.7 (0.2)	5.5 (0.2)	5.8 (0.2)	5.6 (0.2)	7.1 (0.4)	7.1 (0.3)	7.5 (0.6)	7.6 (1.0)	8.3 (0.4)	8.3 (0.4)	8.7 (1.1)	8.9 (1.8)	8.8 (0.5)	8.7 (0.4)	9.3 (1.3)	9.5 (2.1)
Batemans Bay	4.9 (0.2)	4.9 (0.2)	5.3 (0.1)	5.3 ⁵ (0.1) ⁵	6.3 (0.4)	6.4 (0.3)	6.8 (0.5)	7.3 (0.5)	7.3 (0.5)	7.4 (0.4)	7.9 (1.0)	8.9 (0.9)	7.7 (0.5)	7.8 (0.4)	8.4 (1.3)	9.6 (1.2)
Eden	5.4 (0.2)	5.7 (0.2)	5.9 (0.2)	5.8 (0.2)	7.0 (0.4)	7.7 (0.4)	7.8 (0.8)	7.9 (0.8)	8.1 (0.4)	9.1 (0.5)	9.2 (1.3)	9.4 (1.4)	8.5 (0.5)	9.6 (0.6)	9.7 (1.5)	10.1 (1.6)

1. Shand *et al* (2011) based on measured buoy data available at that time. 90% ± confidence intervals presented in brackets.
2. Glatz *et al* (2017) based on measured buoy data available at that time. 90% ± confidence intervals presented in brackets.
3. Baird (2024) based on measured buoy data available at that time. 95% ± confidence intervals presented in brackets.
4. Baird (2024) 67-year hindcast data set. 95% ± confidence intervals presented in brackets.
5. Value taken from Baird (2024) analysis of measured buoy data as 67-year POT value selected for EVA distribution fitting is greater than 1-year ARI return period.

4.2.2 Comparison to other NSW Hindcast Data Sets

Comparisons of extreme wave climate at the NSW offshore buoy locations using measured and hindcast data sets have been presented in previous studies including Cardno (2012) and Shand *et al* (2011). Shand *et al* (2011) used lower resolution spatial and temporal resolution hindcast data sets available in the form of a 13-year NOAA Wavewatch-III (1997 to 2009) data set and a 45-year ERA-40 hindcast data set (1957 to 2002). The EVA of both those hindcasts resulted variable comparisons to the EVA of the measured wave buoy data sets. In general, the ERA-40 data set generated significantly lower estimates of extreme wave heights compared to the buoy data whereas the results from the NOAA Wavewatch-III data was more variable with instances of good agreement in the 100-year ARI wave heights between hindcast and measured data, to locations where the estimates derived from the NOAA Wavewatch-III data set were significantly larger or smaller than the measured data sets. However, the NOAA Wavewatch-III data set had significant uncertainty in the 100-year ARI wave height estimates owing to the short duration of the data set analysed in Shand *et al* (2011).

Cardno (2012) had a longer duration storm data set for the Port Kembla and Sydney buoy locations between 1979 and 2010 using a similar WW3 model grid set to Baird (2024), higher resolution NSW hindcast model. Cardno (2012) presents hindcast estimates of 100-year ARI wave heights at Port Kembla and Sydney buoy locations that were comparable to the EVA of the omni-directional wave height using the measured data sets available at those sites. For example, Cardno (2012) estimated 100-year ARI wave heights of 9.1 m and 9.0 m for Sydney and Port Kembla respectively, compared to 10.2 m and 9.5 m respectively from the 67-year hindcast presented in this report. The additional storm data on the 67-year hindcast, including the larger events such as May 1974 that are included in the 67-year hindcast, but were not included in the Cardno (2012) data set is the primary reason for the increased extreme wave heights from this study. The additional 14-years of measured and hindcast wave data included in this study, compared to the Cardno (2012) study which only had measured and hindcast data to the end of 2009 also contributes to the higher extreme wave heights calculated in this study, compared to Cardno (2012).

Overall, the 67-year hindcast data set used for the EVA in this study estimates larger 50 and 100-year ARI wave heights compared to earlier hindcast data sets for the NSW coastline. The good statistical and time series validation of the 67-year hindcast compared to the measured buoy data presented in Baird (2024), and the generally good agreement in the EVA for the measured data and the hindcast data concurrent with the measured buoy record presented in Section 3.1 provide confidence that the latest NSW hindcast data is a reliable basis to estimate extreme value wave statistics along the NSW coastline.

4.3 Recommendations for Further Studies

The following items, which are beyond the scope of this project, are recommended with respect to deepwater wave climate using the new 67-year continuous hindcast:

- Analyse the deepwater extreme wave height climate along the NSW coastline and compare results to earlier studies, for example Cardno (2012), which indicated that the deepwater wave climate offshore of the Newcastle and Hunter coastlines was the most severe.
- Further analysis and investigation of the hindcast wave data set between Newcastle and Crowdy Head is recommended. The EVA completed on the Baird (2024) 67-year wave hindcast for the offshore Crowdy Head location is the least robust and reliable of all the offshore sites analysed. The source(s) of the lower reliability of the Baird (2024) wave hindcast at Crowdy Head for extreme wave conditions are unclear.
- Re-analyse storm duration statistics and return periods (ARI) for wave heights longer duration storm peaks exceeding 1hr-duration thresholds.
- Analyse jointly occurring wave period, wave direction and wind conditions for extreme storm events using the 67-year hindcast (as demonstrated at Bengello Beach in Oliver *et al.*, 2024 using nearshore measured wave data, BOM winds and a long-term shoreline monitoring dataset).

- Analyse the storm energy return period, in a manner similar to Garber et al (2022) and Harley et al (2017) along the whole NSW coastline to assist with understanding of extreme nearshore wave energy and erosion potential.
- Further analysis of the directional wave climate in the 67-year hindcast presented in Baird (2024) to understand potential bias as a result of relatively small directional offsets and the wave direction bins adopted in the hindcast model. The bias corrections to the 67-year hindcast (see Section A.1.3, Baird, 2024) and the EVA of the resulting data set could be refined in future studies.

5. Acknowledgements

The authors express their gratitude to the staff of the NSW Government, Correllink, and Baird Australia for their involvement in data collection, analysis of wave data, and the development and testing of models and web applications crucial to this project.

Funding for this project was provided by the NSW Coastal Reforms package and the NSW Climate Change Fund, which also supported the collection of the NSW Marine LiDAR Topo-Bathy (2018).

We appreciate the contributions of Brad Morris, Michael Kinsela, David Hanslow, and the entire Coast and Marine Team for securing initial project funding, reviewing project outputs, preparing data, and engaging in valuable discussions on methods and datasets. We also thank Mark Kulmar and Matthew Phillips of Manly Hydraulics Laboratory for supplying offshore wave data. This report was reviewed by Tom Doyle, Raimundo Ibaceta Vega, Senior Scientists, Stuart Young, Acting/Principal Estuary Specialist, and David Hanslow, Team Leader - Coast and Marine (NSW DCCEEW), whose feedback was invaluable.

6. References

- Baird Australia (2017). NSW Coastal Wave Model – State Wide Nearshore Wave Transformation Tool. Prepared for Office of Environment and Heritage (NSW). Report Reference: 12359.101.R2.Rev0. 25 January 2017.
- Baird (2024). NSW Nearshore Wave Transformation Tools Validation Report. Prepared for Department of Climate Change, Energy, the Environment and Water (NSW). Report Reference: 12359.201.R1.RevA. 8 April 2024.
- Cardno (2012). “NSW Coastal Waves: Numerical Modelling – Final Report”. Prepared for the NSW Office of Environment and Heritage. Ref LJ2949/R2745. Version 3. September 2012.
- Coles, S. (2001) An Introduction to Statistical Modeling of Extreme Values. Springer Verlag, Berlin. <http://dx.doi.org/10.1007/978-1-4471-3675-0a>.
- Dent J., Kinsela M., Taylor D., Garber S, Treloar D. (2014). “Evaluation of Downscaled Climate Model Outputs for Generating Long-Term Wave Climate Statistics for the NSW Coastline.” 2014 NSW Coastal Conference (Ulladulla, November 2014).
- Glatz M., Fitzhenry M., Kulmar M. (2017). It's Time for an Update - Extreme Waves and Directional Distributions Along the New South Wales Coastline. Paper presented at the 26th New South Wales Coastal Conference, Port Stephens, November 2017.
- Garber S., Taylor D., and Dent J., (2022). Extreme Wave Climate of the New South Wales Coast. Proceedings of 37th International Conference on Coastal Engineering (ICCE 2022). Sydney, Melbourne, 5-9 December 2022.
- Goda (2000). Random Seas and Design of Maritime Structures. Advanced Series on Ocean Engineering – Volume 15. World Scientific, Singapore. ISBN-13 978-981-02-3256-6.
- Hanslow, D.J., Dela-Cruz, J., Morris, B.D., Kinsela, M.A., Foulsham, E., Linklater, M., and Pritchard, T.R. Regional scale coastal mapping to underpin strategic land use planning in south east Australia. Journal of Coastal Research 2016, 75, 987–991.
- Harley, M.D., Turner, I.L., Short, A.D. and Ranasinghe, R. (2010), Interannual variability and controls of the Sydney wave climate. Int. J. Climatol., 30: 1322-1335. <https://doi.org/10.1002/joc.1962>.
- Harley, M.D., Turner, I.L., Kinsela, M.A. et al (2017). Extreme coastal erosion enhanced by anomalous extratropical storm wave direction. Sci Rep 7, 6033 (2017). <https://doi.org/10.1038/s41598-017-05792-1>
- Hersbach H, Bell B, Berrisford P, et al (2020). The ERA5 global reanalysis. Q J R Meteorol Soc. 2020; 146: 1999–2049. <https://doi.org/10.1002/qj.3803>.
- Kinsela M., Taylor D., Treloar D., Dent J., Garber S., Mortlock T., and Goodwin I. (2014). “NSW Coastal Ocean Wave Model: Investigating Spatial and Temporal Variability in Coastal Wave Climates”. Proceedings of 23rd NSW Coastal Conference (11-14 November, Ulladulla).
- Kinsela M., Morris B.D., Linklater M., and Hanslow D.J. (2017). “Second-Pass Assessment of Potential Exposure to Shoreline Change in New South Wales, Australia, Using a Sediment Compartments Framework”. Journal of Marine Science and Engineering, 5(4):61 (2017). <https://doi.org/10.3390/jmse5040061>
- Kinsela, M.A., Morris, B.D., Ingleton, T.C., Doyle, T.B., Sutherland, M.D., Doszpot M.E., Miller, J.J., Holtznagel, S.F., Harley, M.D., Hanslow, D.J., Nearshore wave buoy data from southeastern Australia for coastal research and management. Sci Data 11, 190 (2024). <https://doi.org/10.1038/s41597-023-02865-x>.

Lobeto, H., Semedo, A., Lemos, G. et al. Global coastal wave storminess. *Sci Rep* 14, 3726 (2024). <https://doi.org/10.1038/s41598-024-51420-0>.

MHL (2022). NSW Wave Climate Annual Summary 2020-2021. Prepared for the NSW Department of Planning, Industry and Environment. Report MHL2858. February 2022.

Morris B.D., Foulsham E., Laine R., Wiecek D., and Hanslow D.J., Evaluation of Runup Characteristics on the NSW Coast. *Journal of Coastal Research* 2016, 75, 1187 – 1191. <https://doi.org/10.2112/SI75-238.1>

Naess A and Hungnes B. (2002). "Estimating Confidence Intervals of Long Return Period Design Values by Bootstrapping". *Journal of Offshore and Arctic Engineering*. American Society of Mechanical Engineers.

Oliver, T. S. N., Kinsela, M. A., Doyle, T. B., & McLean, R. F. (2024). Foredune erosion, overtopping and destruction in 2022 at Bengello Beach, southeastern Australia. *Cambridge Prisms: Coastal Futures*, 2, e7. <https://doi.org/10.1017/cft.2024.8>.

Shand, T. D., Goodwin, I. D., Mole, M. A., Carley, J. T., Browning, S., Coghlan, I. R., Harley, M.D., and Peirson, W. L. (2011). NSW Coastal Inundation Hazard Studies: Coastal Storms and Extreme Waves. Water Research Laboratory, Technical Report 2010/16.

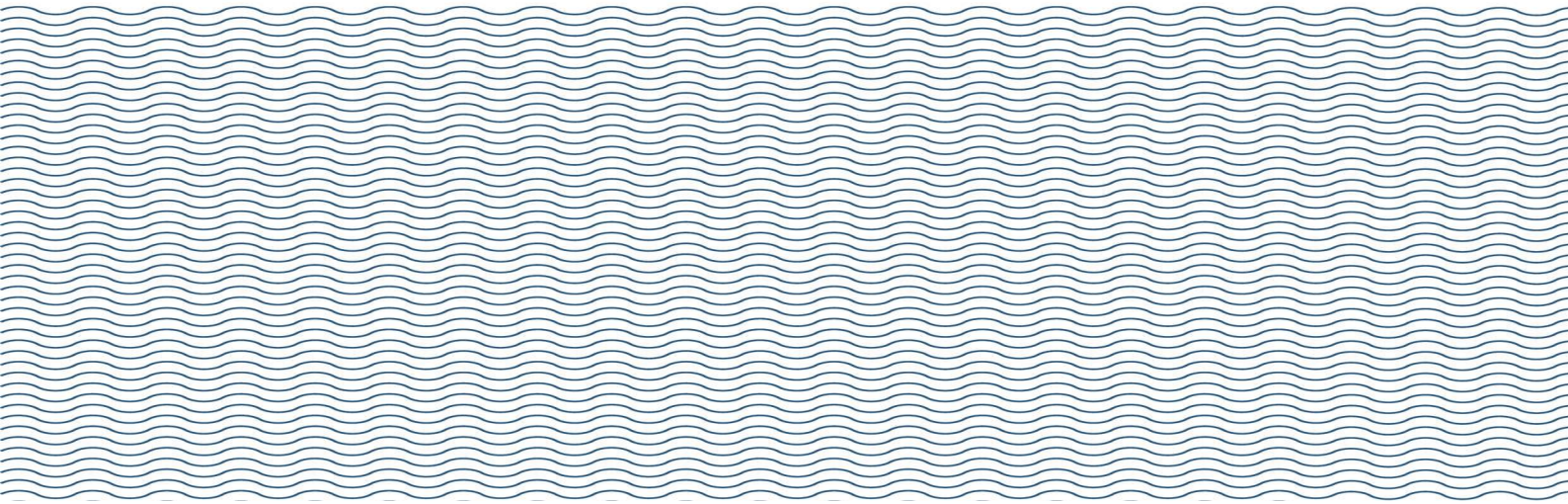
Taylor D. R. (2006) 'Nonlinear Estimation of Extreme Value Model Parameters in Coastal and Ocean Engineering'. Graduate paper from Queen's University, Canada. Course CHEE-824: Non-linear regression. April 2006.

Taylor D.R, Burston A.M, Dent J. D and Garber S. G (2017). East Coast Lows: A Wind, Rainfall and Inundation Hazard Database for NSW. Proceedings of NSW Coastal Conference. Shoal Bay, November 2017.

USACE (2001) "Coastal Engineering Manual". US Army Corp of Engineers. Washington DC, 20314-1000.

van Vledder G, Goda Y, Hawkes P, Mansard E, Martin M, Mathiesen M, Thompson E F and Peltier E (1993). "Case studies of Extreme Wave Analysis: a Comparative Analysis." *Ocean Wave Measurement and Analysis – Proceedings of the Second International Symposium*. New Orleans, Louisiana.

You Z. J., (2007). Extrapolation of extreme wave height with a proper probability distribution function. Australasian Coasts and Ports Conference, 17-20 July Melbourne.



Appendix A

Storm Peaks Summary



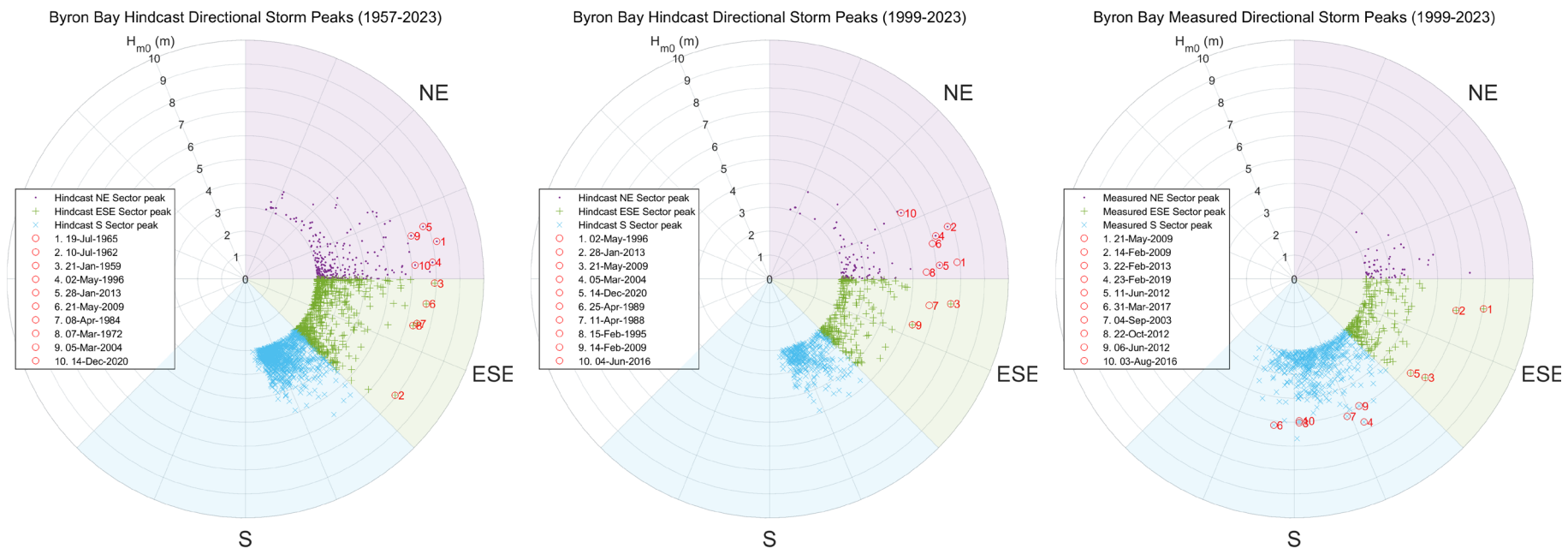


Figure A.1: Byron Bay Storm Peaks Comparison

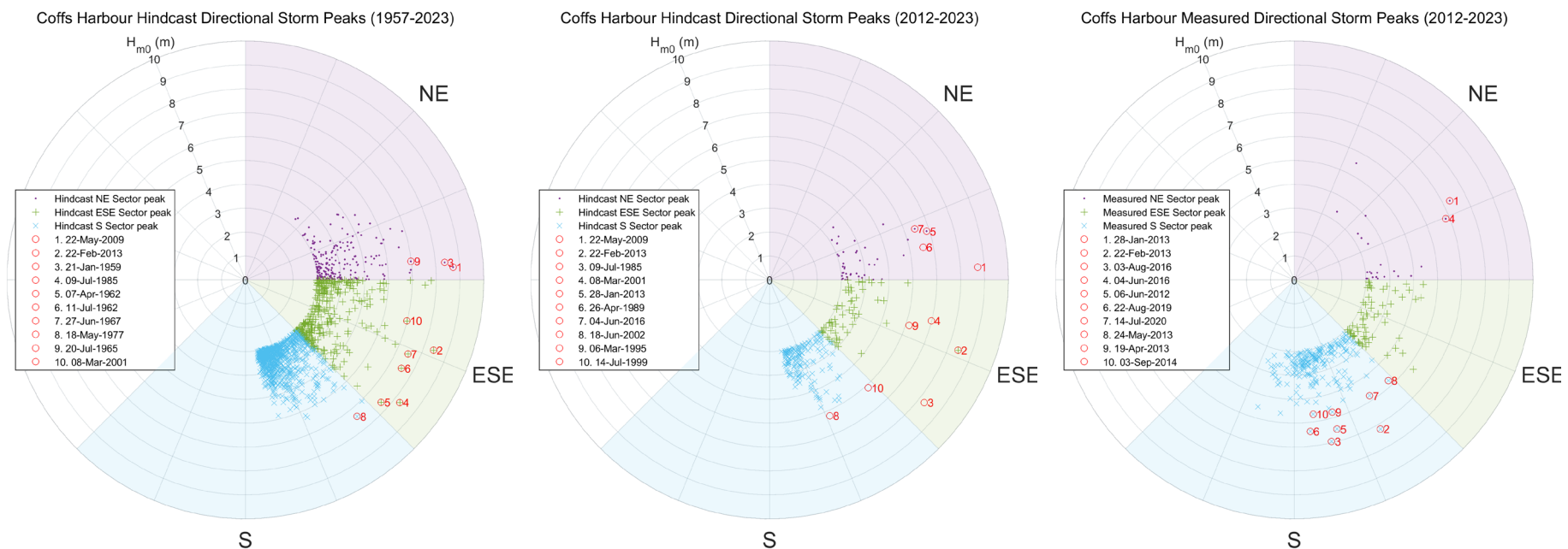


Figure A.2: Coffs Harbour Storm Peaks Comparison

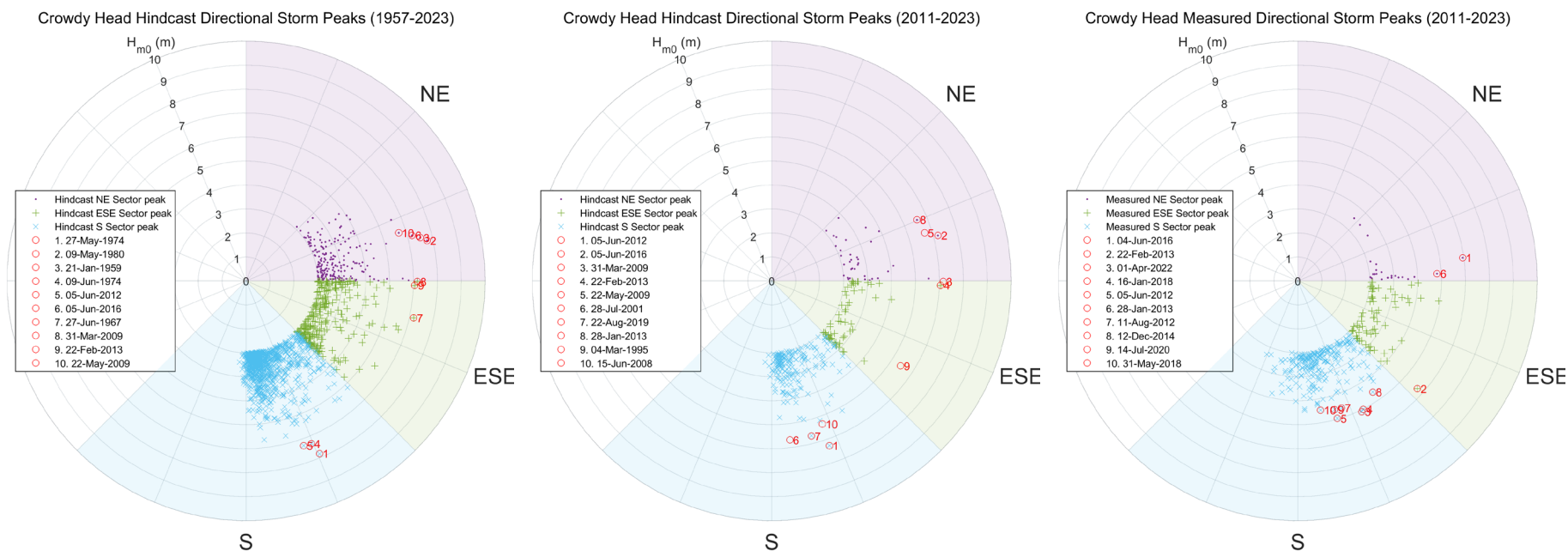


Figure A.3: Crowdy Head Storm Peaks Comparison

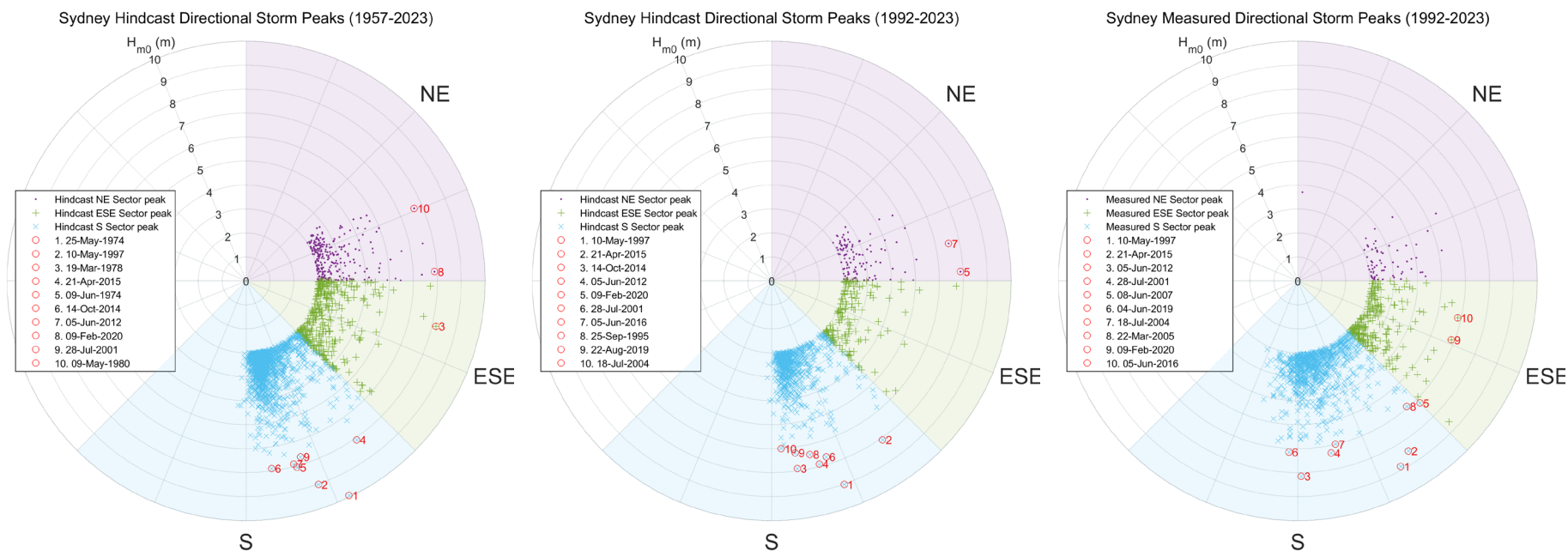


Figure A.4: Sydney Storm Peaks Comparison

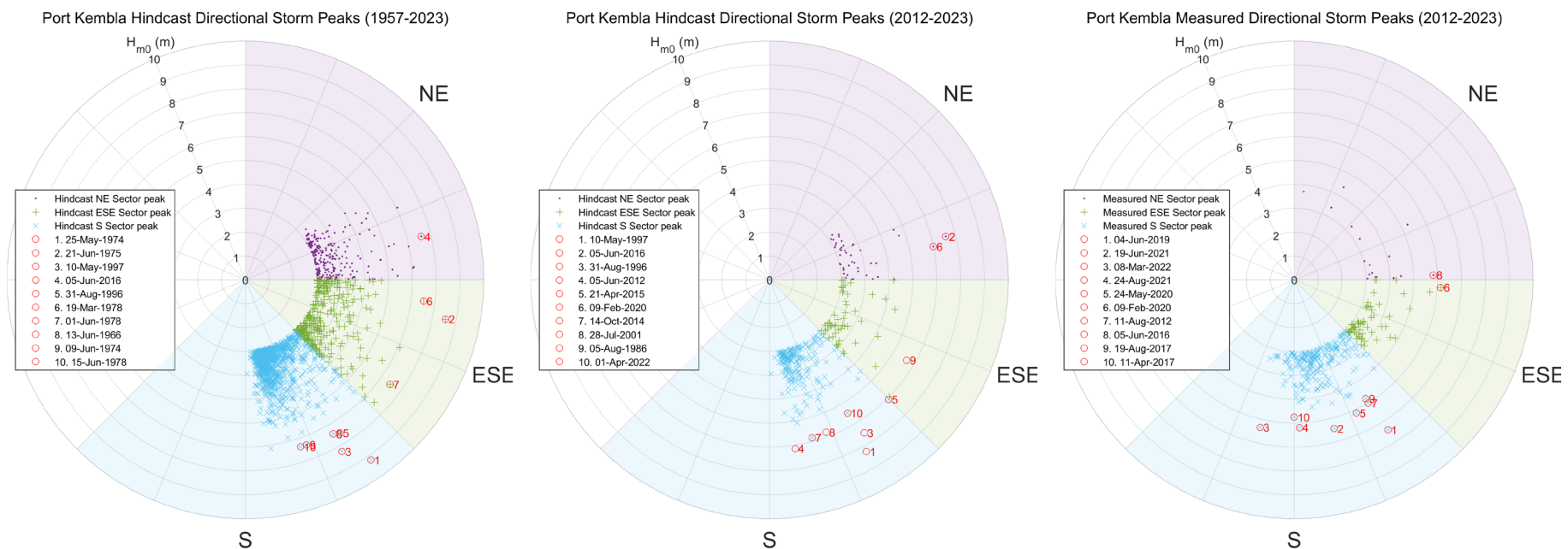


Figure A.5: Port Kembla Storm Peaks Comparison

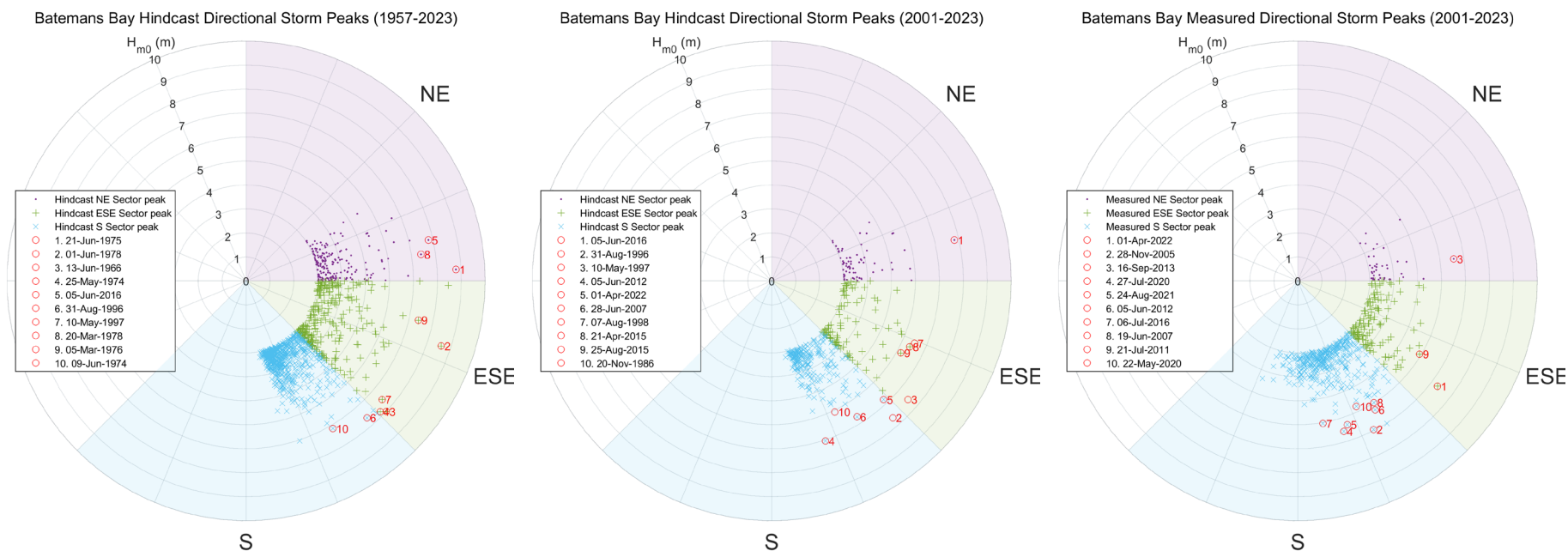


Figure A.6: Batemans Bay Storm Peaks Comparison

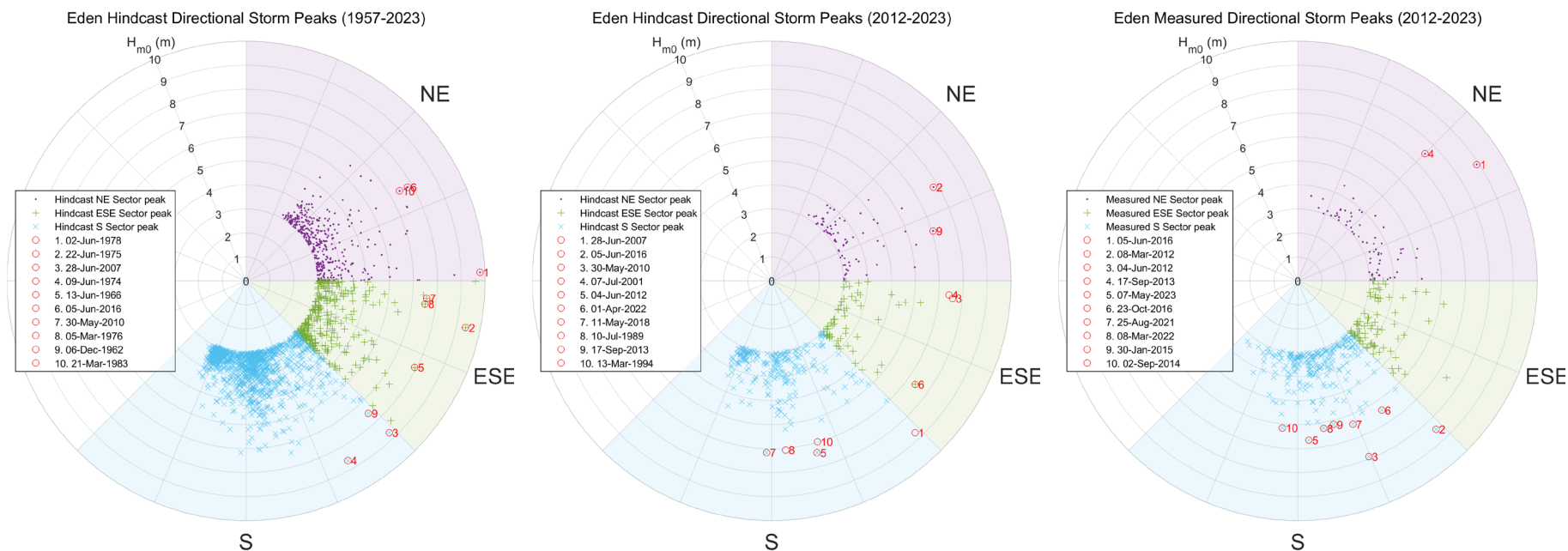
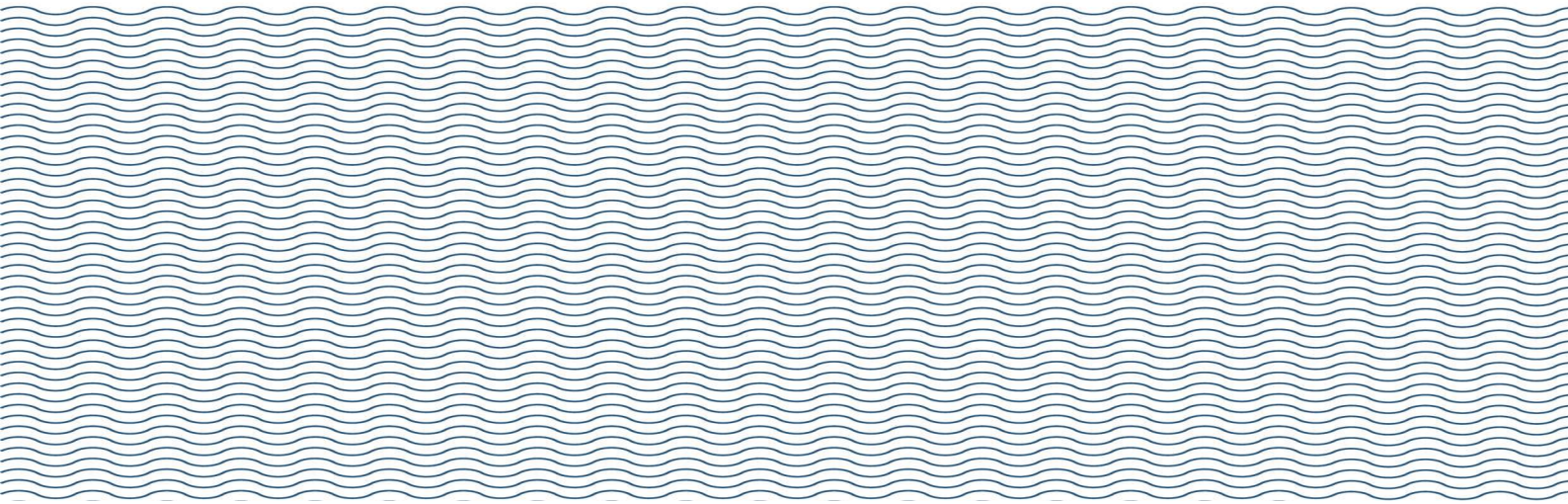


Figure A.7: Eden Storm Peaks Comparison



Appendix B

Extreme Wave Height Analysis Results



B.1 Byron Bay

Extreme Value Analysis - GEV fit **Date Range** **Measured:** **1984 - 2023** refer to Table 2.3
Location **Byron Bay** **Hindcast:** **1957 - 2023**

Extreme Value Analysis - Omnidirectional

ARI (years)	Dataset					
	Hindcast		Measured		Hindcast Concurrent	
	Hm0 (m)	CI (± m)	Hm0 (m)	CI (± m)	Hm0 (m)	CI (± m)
1	5.27	0.09	5.46	0.19	5.19	0.11
2	5.86	0.17	5.85	0.38	5.72	0.26
5	6.65	0.30	6.37	0.69	6.43	0.49
10	7.26	0.41	6.77	0.96	6.99	0.68
20	7.87	0.53	7.17	1.24	7.55	0.90
50	8.69	0.70	7.70	1.64	8.30	1.20
100	9.31	0.84	8.11	1.97	8.87	1.44
200	9.93	0.99	8.51	2.31	9.45	1.69
500	10.76	1.19	9.05	2.77	10.21	2.04

Extreme Value Analysis - GEV fit **Date Range** **Measured:** **1999 - 2023** refer to Table 2.3
Location **Byron Bay** **Hindcast:** **1957 - 2023**

Extreme Value Analysis - North-East Directional Sector (0 - 90 degrees)

ARI (years)	Dataset					
	Hindcast		Measured		Hindcast Concurrent	
	Hm0 (m)	CI (± m)	Hm0 (m)	CI (± m)	Hm0 (m)	CI (± m)
1	4.51	0.06	3.84	0.19	4.23	0.08
2	5.31	0.24	4.45	0.45	4.89	0.29
5	6.28	0.36	5.30	0.95	5.86	0.60
10	6.98	0.45	5.96	1.42	6.63	0.87
20	7.67	0.57	6.63	1.95	7.43	1.16
50	8.56	0.78	7.53	2.72	8.51	1.57
100	9.23	0.96	8.21	3.34	9.35	1.91
200	9.89	1.16	8.91	4.00	10.20	2.27
500	10.75	1.45	9.83	4.91	11.35	2.77

Extreme Value Analysis - East Southeast Directional Sector (90 - 135 degrees)

ARI (years)	Dataset					
	Hindcast		Measured		Hindcast Concurrent	
	Hm0 (m)	CI (± m)	Hm0 (m)	CI (± m)	Hm0 (m)	CI (± m)
1	4.77	0.11	4.72	0.26	4.77	0.22
2	5.33	0.28	5.27	0.61	5.21	0.41
5	6.07	0.55	6.06	1.16	5.74	0.76
10	6.64	0.79	6.69	1.63	6.10	1.07
20	7.20	1.04	7.35	2.14	6.44	1.40
50	7.95	1.40	8.24	2.88	6.88	1.85
100	8.52	1.69	8.93	3.47	7.19	2.21
200	9.08	1.98	9.64	4.09	7.49	2.58
500	9.84	2.39	10.59	4.94	7.88	3.09

Extreme Value Analysis - South Directional Sector (135 - 225 degrees)

ARI (years)	Dataset					
	Hindcast		Measured		Hindcast Concurrent	
	Hm0 (m)	CI (± m)	Hm0 (m)	CI (± m)	Hm0 (m)	CI (± m)
1	5.15	0.18	5.29	0.19	5.17	0.15
2	5.53	0.29	5.68	0.28	5.55	0.20
5	6.02	0.47	6.19	0.43	6.02	0.30
10	6.38	0.61	6.56	0.56	6.36	0.40
20	6.74	0.76	6.94	0.70	6.69	0.50
50	7.21	0.98	7.42	0.90	7.11	0.65
100	7.57	1.14	7.79	1.05	7.43	0.78
200	7.92	1.32	8.15	1.22	7.74	0.91
500	8.38	1.55	8.62	1.44	8.14	1.08

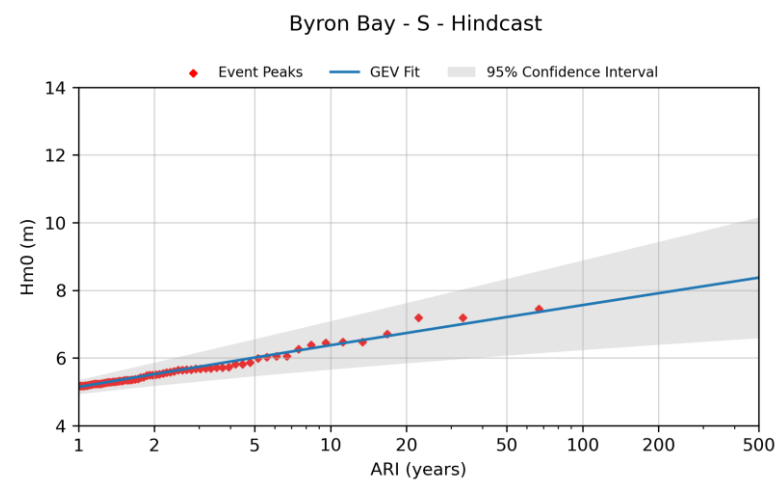
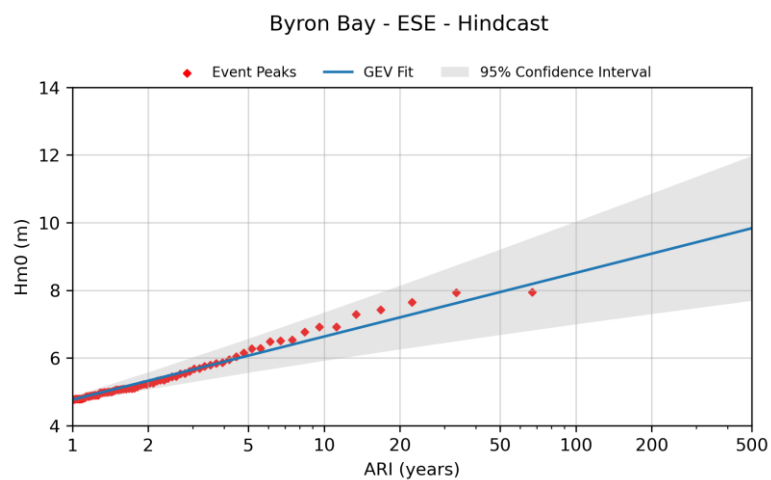
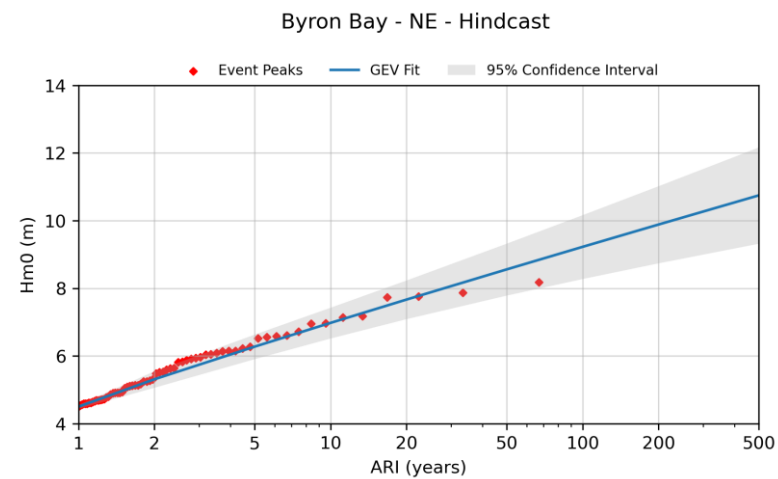
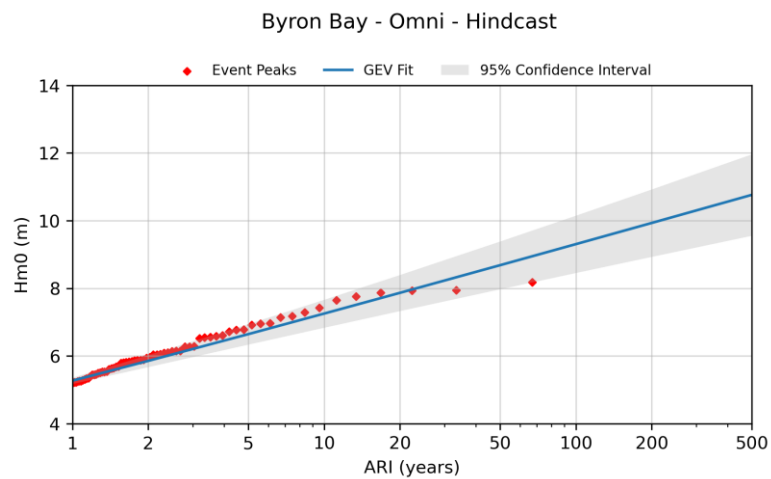


Figure B.1: Extreme Wave Height Analysis Results for Hindcast 1957-2023, Storm Peaks and GEV Fit – Byron Bay

B.2 Coffs Harbour

Extreme Value Analysis - GEV fit **Date Range** **Measured:** **1984 - 2023** refer to Table 2.3
Location **Coffs Harbour** **Hindcast:** **1957 - 2023**

Extreme Value Analysis - Omnidirectional

ARI (years)	Dataset					
	Hindcast		Measured		Hindcast Concurrent	
	Hm0 (m)	CI (± m)	Hm0 (m)	CI (± m)	Hm0 (m)	CI (± m)
1	5.27	0.18	5.63	0.16	5.28	0.10
2	5.84	0.38	6.10	0.22	5.78	0.38
5	6.62	0.69	6.69	0.33	6.45	0.89
10	7.22	0.95	7.11	0.45	6.95	1.34
20	7.83	1.22	7.52	0.59	7.46	1.83
50	8.65	1.60	8.04	0.79	8.12	2.54
100	9.27	1.90	8.43	0.95	8.63	3.11
200	9.90	2.21	8.81	1.12	9.13	3.71
500	10.73	2.64	9.31	1.36	9.80	4.54

Extreme Value Analysis - GEV fit **Date Range** **Measured: 2012 - 2023** refer to Table 2.3
Location **Coffs Harbour** **Hindcast: 1957 - 2023**

Extreme Value Analysis - North-East Directional Sector (0 - 90 degrees)

ARI (years)	Dataset					
	Hindcast		Measured		Hindcast Concurrent	
	Hm0 (m)	CI (± m)	Hm0 (m)	CI (± m)	Hm0 (m)	CI (± m)
1	4.12	0.18	3.77	0.23	4.00	0.33
2	4.86	0.30	4.59	0.53	4.74	0.52
5	5.85	0.50	5.79	0.95	5.77	0.84
10	6.59	0.67	6.76	1.31	6.57	1.13
20	7.34	0.86	7.77	1.72	7.39	1.47
50	8.34	1.14	9.15	2.36	8.48	1.96
100	9.09	1.36	10.22	2.92	9.32	2.37
200	9.84	1.60	11.31	3.55	10.16	2.79
500	10.84	1.92	12.79	4.48	11.29	3.39

Extreme Value Analysis - East Southeast Directional Sector (90 - 135 degrees)

ARI (years)	Dataset					
	Hindcast		Measured		Hindcast Concurrent	
	Hm0 (m)	CI (± m)	Hm0 (m)	CI (± m)	Hm0 (m)	CI (± m)
1	4.39	0.12	4.38	0.26	3.99	58.04
2	5.13	0.21	4.86	0.37	4.46	0.63
5	6.16	0.35	5.52	0.56	5.24	1.56
10	6.96	0.48	6.03	0.74	5.90	2.43
20	7.77	0.61	6.56	0.95	6.60	3.44
50	8.86	0.81	7.26	1.27	7.58	4.96
100	9.70	0.98	7.80	1.53	8.36	6.24
200	10.54	1.15	8.35	1.81	9.17	7.64
500	11.67	1.40	9.07	2.21	10.27	9.66

Extreme Value Analysis - South Directional Sector (135 - 225 degrees)

ARI (years)	Dataset					
	Hindcast		Measured		Hindcast Concurrent	
	Hm0 (m)	CI (± m)	Hm0 (m)	CI (± m)	Hm0 (m)	CI (± m)
1	5.53	0.10	5.37	0.26	5.47	0.37
2	6.01	0.20	5.85	0.38	5.96	0.35
5	6.58	0.37	6.54	0.59	6.65	0.48
10	7.00	0.53	7.09	0.84	7.18	0.76
20	7.41	0.71	7.64	1.13	7.72	1.13
50	7.92	0.98	8.39	1.59	8.45	1.69
100	8.31	1.19	8.96	1.96	9.00	2.16
200	8.69	1.42	9.55	2.37	9.57	2.65
500	9.18	1.72	10.32	2.93	10.31	3.34

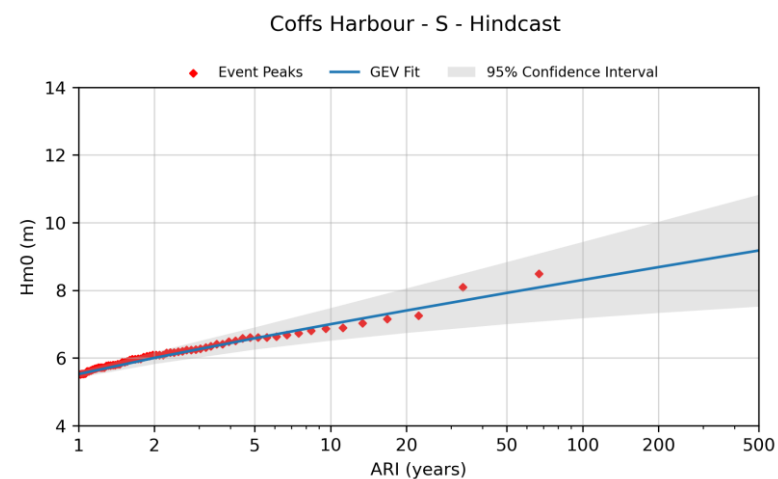
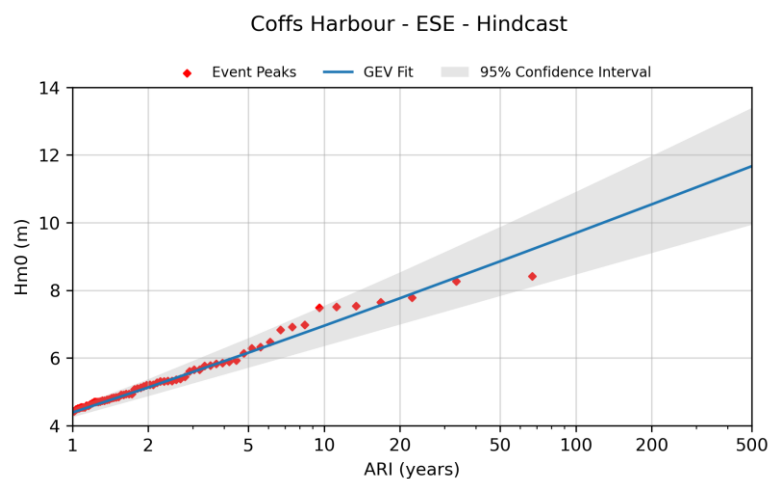
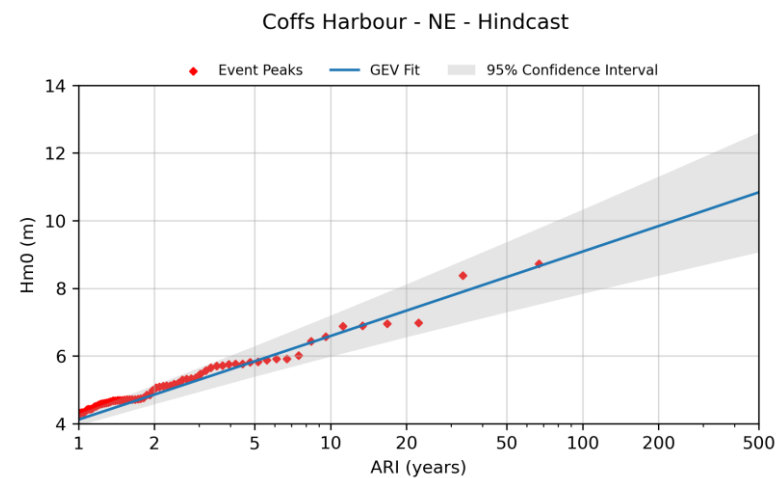
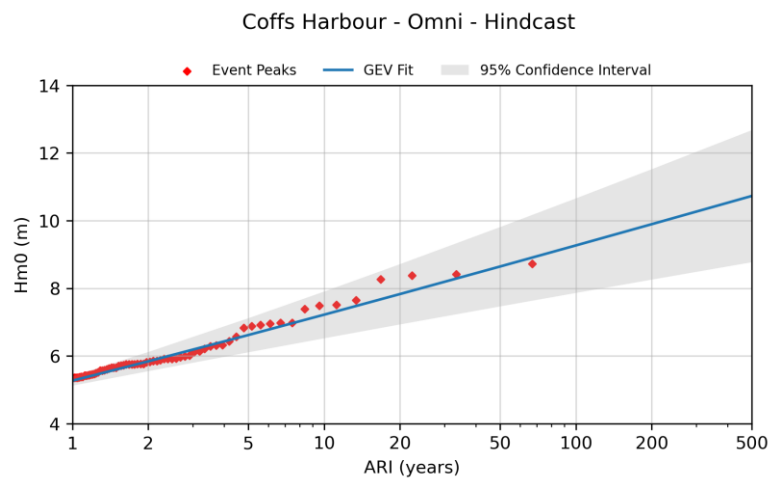


Figure B.2: Extreme Wave Height Analysis Results for Hindcast 1957-2023, Storm Peaks and GEV Fit – Coffs Harbour

B.3 Crowdy Head

Extreme Value Analysis - GEV fit **Date Range** **Measured:** **1985 - 2023** refer to Table 2.3
Location **Crowdy Head** **Hindcast:** **1957 - 2023**

Extreme Value Analysis - Omnidirectional

ARI (years)	Dataset					
	Hindcast		Measured		Hindcast Concurrent	
	Hm0 (m)	CI (± m)	Hm0 (m)	CI (± m)	Hm0 (m)	CI (± m)
1	5.45	0.08	5.62	0.11	5.34	0.06
2	5.95	0.16	6.07	0.22	5.85	0.19
5	6.53	0.26	6.67	0.32	6.43	0.27
10	6.94	0.36	7.13	0.45	6.84	0.37
20	7.34	0.48	7.59	0.63	7.23	0.50
50	7.84	0.66	8.20	0.91	7.74	0.73
100	8.21	0.81	8.66	1.14	8.11	0.93
200	8.57	0.97	9.12	1.40	8.48	1.14
500	9.03	1.19	9.74	1.75	8.96	1.45

Extreme Value Analysis - GEV fit **Date Range** **Measured:** **2011 - 2023** refer to Table 2.3
Location **Crowdy Head** **Hindcast:** **1957 - 2023**

Extreme Value Analysis - North-East Directional Sector (0 - 90 degrees)

ARI (years)	Dataset					
	Hindcast		Measured		Hindcast Concurrent	
	Hm0 (m)	CI (± m)	Hm0 (m)	CI (± m)	Hm0 (m)	CI (± m)
1						
2	4.66	0.07	4.26	0.41	4.63	0.61
5	5.44	0.31	5.20	0.94	5.61	0.83
10	6.06	0.53	6.04	1.44	6.38	1.11
20	6.71	0.77	6.96	2.03	7.17	1.49
50	7.58	1.14	8.27	2.94	8.24	2.10
100	8.26	1.44	9.32	3.76	9.06	2.63
200	8.94	1.76	10.41	4.71	9.89	3.20
500	9.85	2.22	11.91	6.23	11.00	4.01

Extreme Value Analysis - East Southeast Directional Sector (90 - 135 degrees)

ARI (years)	Dataset					
	Hindcast		Measured		Hindcast Concurrent	
	Hm0 (m)	CI (± m)	Hm0 (m)	CI (± m)	Hm0 (m)	CI (± m)
1			4.48	0.25		
2	4.61	0.16	4.96	0.45	4.23	0.41
5	5.37	0.28	5.59	0.83	4.90	0.92
10	5.97	0.37	6.08	1.19	5.45	1.51
20	6.57	0.49	6.57	1.59	6.02	2.22
50	7.39	0.70	7.22	2.17	6.80	3.33
100	8.01	0.89	7.71	2.64	7.41	4.30
200	8.64	1.10	8.20	3.13	8.03	5.42
500	9.47	1.41	8.86	3.81	8.87	7.16

Extreme Value Analysis - South Directional Sector (135 - 225 degrees)

ARI (years)	Dataset					
	Hindcast		Measured		Hindcast Concurrent	
	Hm0 (m)	CI (± m)	Hm0 (m)	CI (± m)	Hm0 (m)	CI (± m)
1	5.12	0.09	5.20	0.20	5.02	0.18
2	5.58	0.16	5.53	0.26	5.50	0.33
5	6.21	0.28	5.95	0.40	6.18	0.57
10	6.68	0.38	6.25	0.54	6.72	0.78
20	7.16	0.50	6.54	0.70	7.28	1.02
50	7.79	0.67	6.92	0.92	8.03	1.37
100	8.27	0.81	7.19	1.10	8.62	1.65
200	8.75	0.95	7.46	1.29	9.21	1.96
500	9.38	1.15	7.81	1.54	10.00	2.39

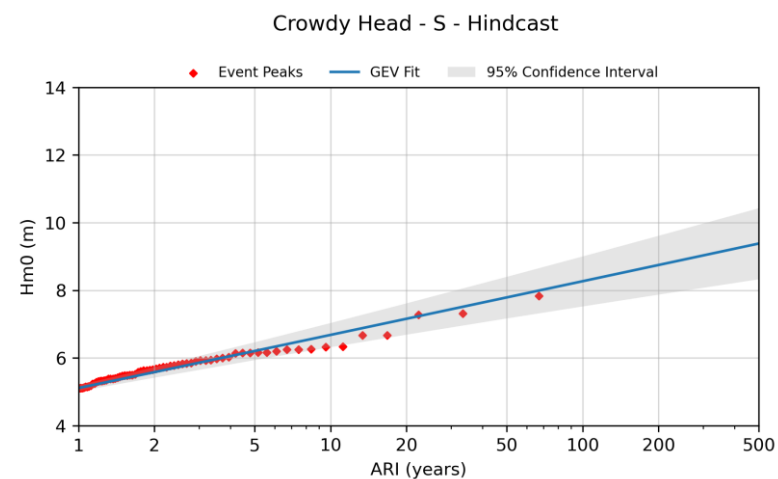
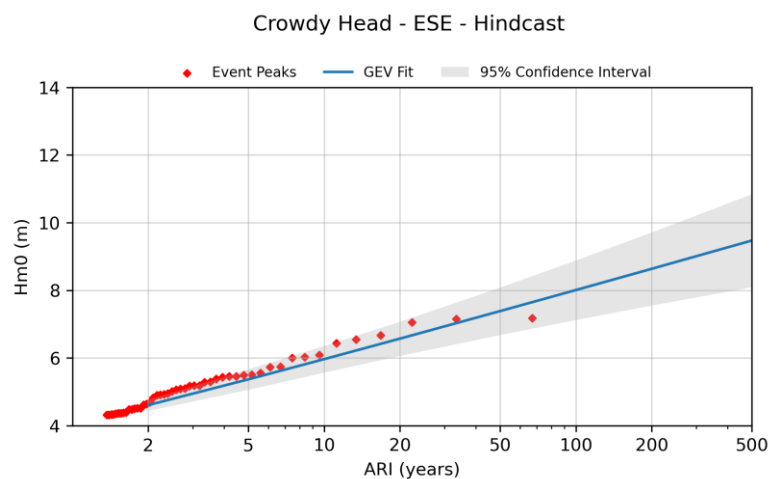
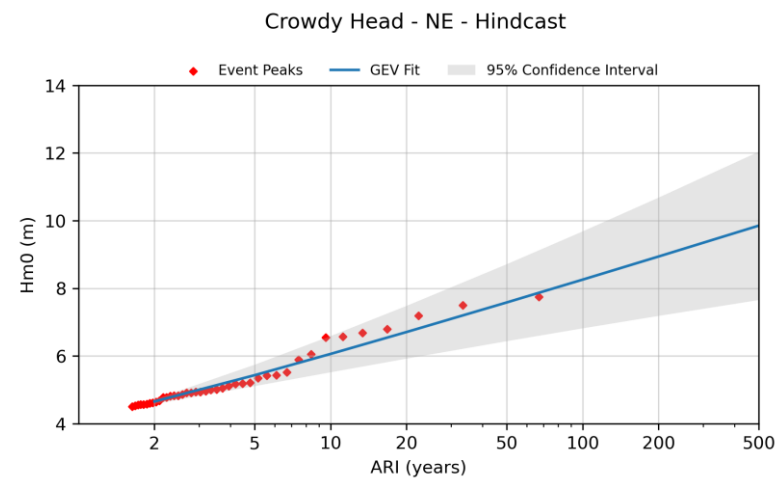
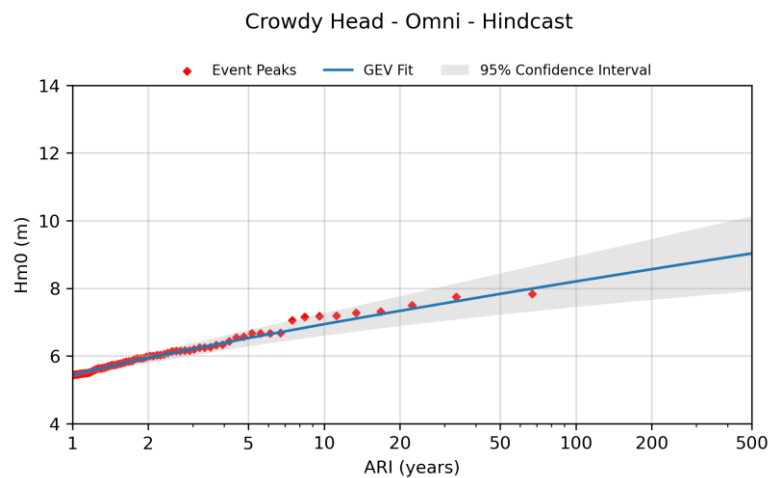


Figure B.3: Extreme Wave Height Analysis Results for Hindcast 1957-2023, Storm Peaks and GEV Fit – Crowdy Head

B.4 Sydney

Extreme Value Analysis - GEV fit **Date Range** **Measured:** **1987 - 2023** refer to Table 2.3
Location **Sydney** **Hindcast:** **1957 - 2023**

Extreme Value Analysis - Omnidirectional

ARI (years)	Dataset					
	Hindcast		Measured		Hindcast Concurrent	
	Hm0 (m)	CI (± m)	Hm0 (m)	CI (± m)	Hm0 (m)	CI (± m)
1	5.98	0.16	6.18	0.18	5.93	0.19
2	6.60	0.33	6.71	0.24	6.51	0.31
5	7.43	0.61	7.37	0.38	7.23	0.53
10	8.05	0.85	7.86	0.53	7.75	0.73
20	8.68	1.11	8.33	0.71	8.27	0.95
50	9.52	1.48	8.94	0.97	8.93	1.27
100	10.15	1.77	9.39	1.18	9.43	1.53
200	10.78	2.07	9.84	1.40	9.91	1.80
500	11.62	2.48	10.42	1.71	10.55	2.18

Extreme Value Analysis - GEV fit **Date Range** **Measured:** **1992 - 2023** refer to Table 2.3
Location **Sydney** **Hindcast:** **1957 - 2023**

Extreme Value Analysis - North-East Directional Sector (0 - 90 degrees)

ARI (years)	Dataset					
	Hindcast		Measured		Hindcast Concurrent	
	Hm0 (m)	CI (± m)	Hm0 (m)	CI (± m)	Hm0 (m)	CI (± m)
1	3.59	0.04	3.59	0.08		
2	4.18	0.17	4.28	0.33	4.00	0.20
5	4.98	0.31	5.09	0.41	4.83	0.46
10	5.58	0.43	5.67	0.52	5.49	0.68
20	6.19	0.57	6.24	0.71	6.16	0.93
50	6.99	0.78	6.97	1.04	7.07	1.30
100	7.60	0.95	7.51	1.33	7.77	1.60
200	8.22	1.14	8.04	1.65	8.47	1.93
500	9.02	1.40	8.74	2.11	9.41	2.38

Extreme Value Analysis - East Southeast Directional Sector (90 - 135 degrees)

ARI (years)	Dataset					
	Hindcast		Measured		Hindcast Concurrent	
	Hm0 (m)	CI (± m)	Hm0 (m)	CI (± m)	Hm0 (m)	CI (± m)
1						
2	5.56	0.06	5.52	0.22	5.20	0.23
5	6.32	0.31	6.34	0.47	6.14	0.50
10	6.94	0.52	6.97	0.70	6.87	0.71
20	7.58	0.76	7.61	0.95	7.60	1.01
50	8.44	1.10	8.46	1.34	8.58	1.53
100	9.10	1.38	9.11	1.66	9.32	1.98
200	9.77	1.67	9.75	2.00	10.07	2.47
500	10.67	2.08	10.62	2.48	11.07	3.17

Extreme Value Analysis - South Directional Sector (135 - 225 degrees)

ARI (years)	Dataset					
	Hindcast		Measured		Hindcast Concurrent	
	Hm0 (m)	CI (± m)	Hm0 (m)	CI (± m)	Hm0 (m)	CI (± m)
1	5.79	0.15	6.07	0.23	5.78	0.18
2	6.39	0.33	6.64	0.36	6.41	0.29
5	7.16	0.65	7.38	0.59	7.21	0.47
10	7.73	0.92	7.93	0.79	7.79	0.66
20	8.29	1.22	8.47	1.02	8.36	0.87
50	9.02	1.65	9.19	1.35	9.09	1.18
100	9.57	1.99	9.73	1.61	9.64	1.44
200	10.11	2.34	10.27	1.89	10.18	1.72
500	10.83	2.83	10.97	2.26	10.89	2.10

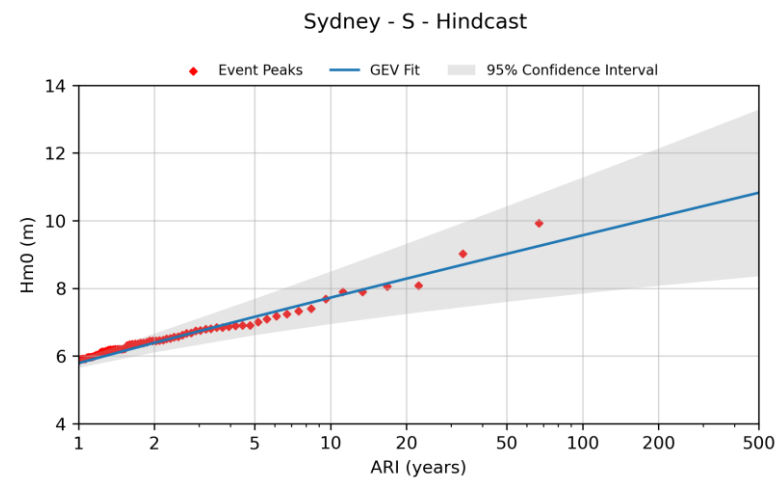
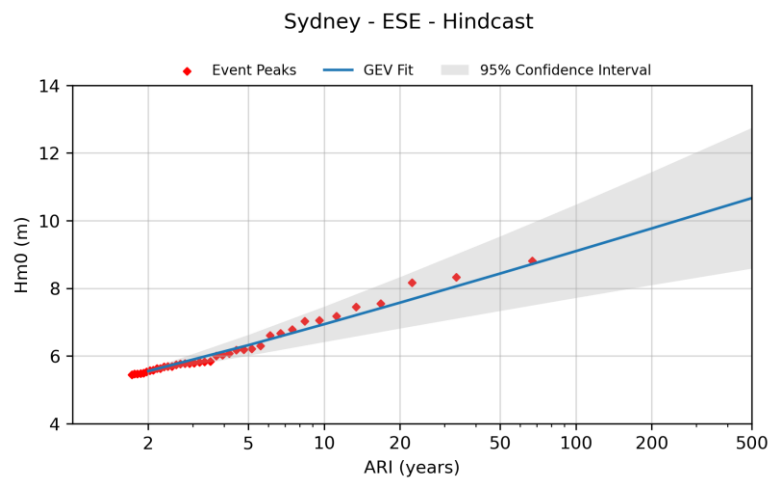
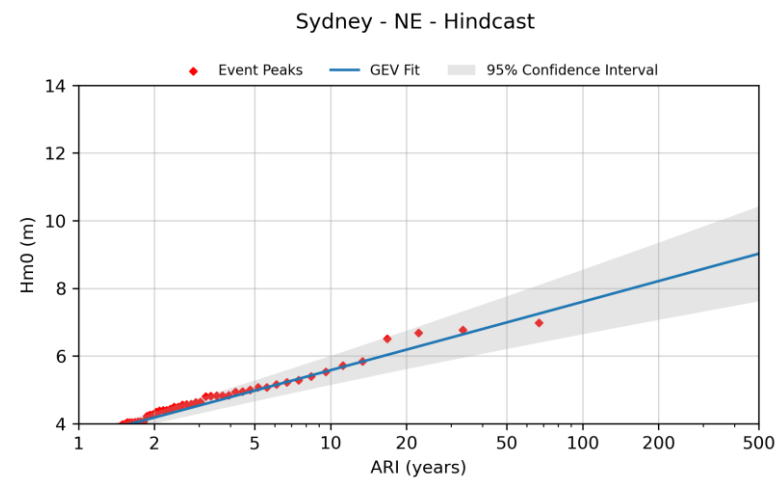
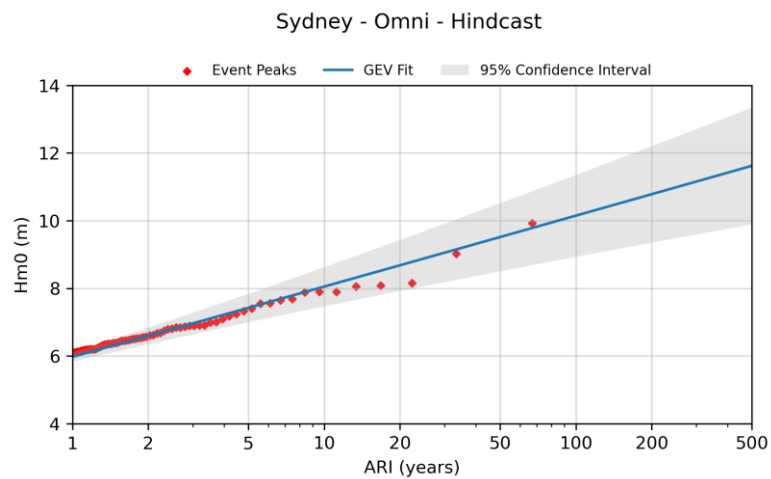


Figure B.4: Extreme Wave Height Analysis Results for Hindcast 1957-2023, Storm Peaks and GEV Fit – Sydney

B.5 Port Kembla

Extreme Value Analysis - GEV fit **Date Range** **Measured: 1984 - 2023** refer to Table 2.3
Location **Port Kembla** **Hindcast: 1957 - 2023**

Extreme Value Analysis - Omnidirectional

ARI (years)	Dataset					
	Hindcast		Measured		Hindcast Concurrent	
	Hm0 (m)	CI (± m)	Hm0 (m)	CI (± m)	Hm0 (m)	CI (± m)
1	5.62	0.18	5.78	0.16	5.78	0.16
2	6.20	0.37	6.30	0.27	6.30	0.27
5	6.96	0.66	6.99	0.46	6.99	0.46
10	7.55	0.91	7.52	0.62	7.52	0.62
20	8.13	1.17	8.04	0.81	8.04	0.81
50	8.91	1.54	8.74	1.07	8.74	1.07
100	9.50	1.83	9.27	1.29	9.27	1.29
200	10.09	2.13	9.80	1.52	9.80	1.52
500	10.88	2.54	10.50	1.83	10.50	1.83

Extreme Value Analysis - GEV fit **Date Range** **Measured:** **2012 - 2023** refer to Table 2.3
Location **Port Kembla** **Hindcast:** **1957 - 2023**

Extreme Value Analysis - North-East Directional Sector (0 - 90 degrees)

ARI (years)	Dataset					
	Hindcast		Measured		Hindcast Concurrent	
	Hm0 (m)	CI (± m)	Hm0 (m)	CI (± m)	Hm0 (m)	CI (± m)
1	3.52	0.10	3.52	0.27	3.19	0.28
2	4.09	0.20	4.11	0.46	3.80	0.58
5	4.91	0.35	4.95	0.77	4.74	1.05
10	5.56	0.48	5.61	1.05	5.51	1.47
20	6.22	0.62	6.29	1.35	6.33	1.96
50	7.13	0.82	7.21	1.79	7.46	2.71
100	7.82	0.99	7.92	2.14	8.36	3.37
200	8.53	1.17	8.65	2.51	9.28	4.10
500	9.49	1.42	9.62	3.03	10.54	5.21

Extreme Value Analysis - East Southeast Directional Sector (90 - 135 degrees)

ARI (years)	Dataset					
	Hindcast		Measured		Hindcast Concurrent	
	Hm0 (m)	CI (± m)	Hm0 (m)	CI (± m)	Hm0 (m)	CI (± m)
1	4.34	0.11	4.19	0.26	4.19	0.26
2	4.98	0.30	4.73	0.48	4.73	0.48
5	5.82	0.63	5.49	0.83	5.49	0.83
10	6.45	0.91	6.09	1.13	6.09	1.13
20	7.09	1.22	6.72	1.46	6.72	1.46
50	7.93	1.65	7.57	1.94	7.57	1.94
100	8.57	2.00	8.22	2.34	8.22	2.34
200	9.21	2.37	8.89	2.76	8.89	2.76
500	10.05	2.87	9.79	3.36	9.79	3.36

Extreme Value Analysis - South Directional Sector (135 - 225 degrees)

ARI (years)	Dataset					
	Hindcast		Measured		Hindcast Concurrent	
	Hm0 (m)	CI (± m)	Hm0 (m)	CI (± m)	Hm0 (m)	CI (± m)
1	5.32	0.12	5.48	0.37	5.48	0.37
2	5.85	0.30	6.01	0.55	6.01	0.55
5	6.57	0.64	6.73	0.82	6.73	0.82
10	7.12	0.93	7.28	1.04	7.28	1.04
20	7.68	1.25	7.83	1.28	7.83	1.28
50	8.42	1.71	8.57	1.61	8.57	1.61
100	8.98	2.08	9.14	1.87	9.14	1.87
200	9.55	2.47	9.71	2.14	9.71	2.14
500	10.31	3.00	10.46	2.52	10.46	2.52

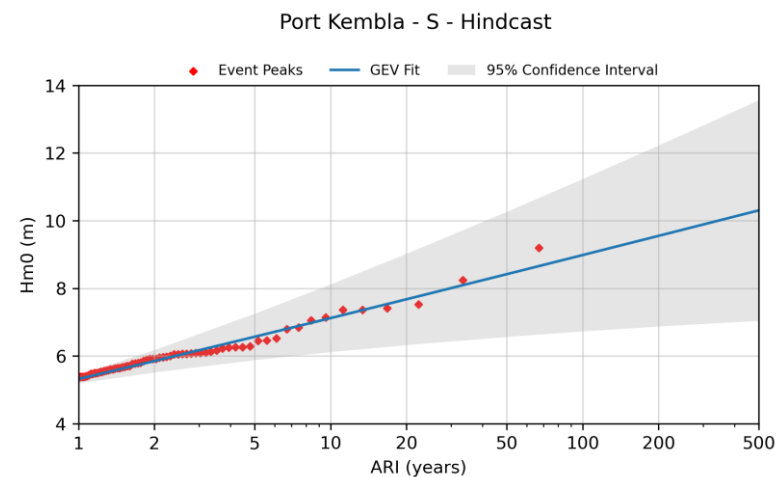
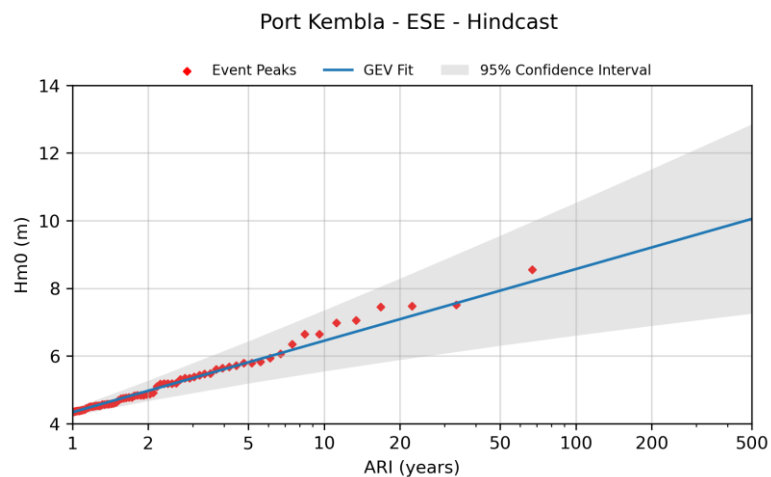
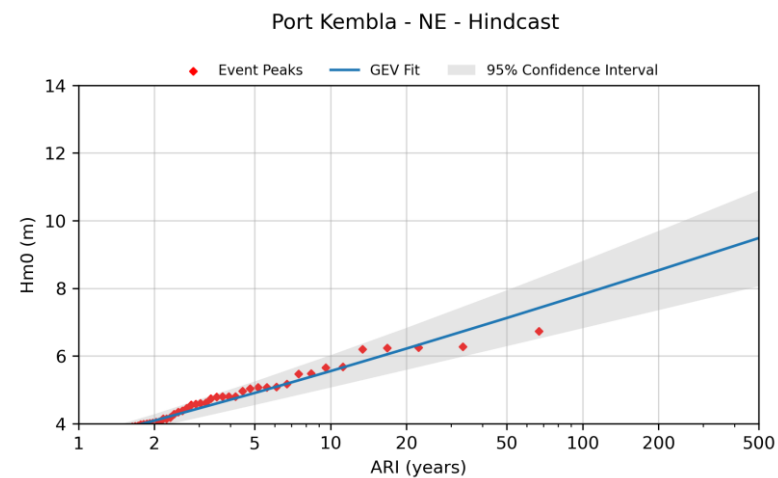
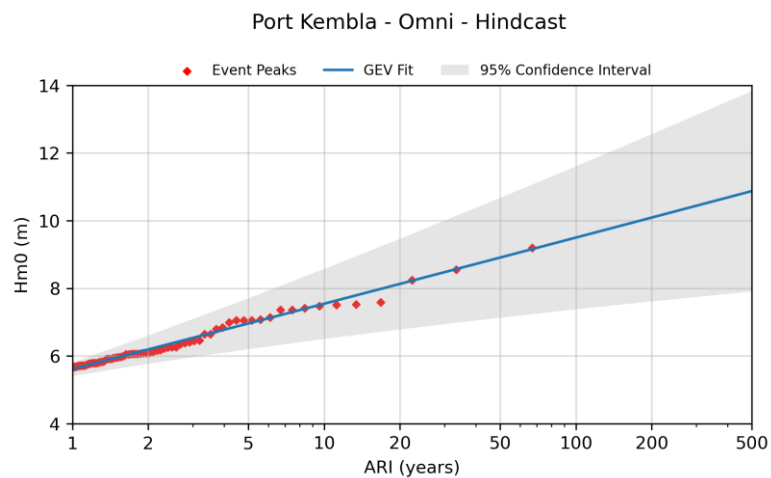


Figure B.5: Extreme Wave Height Analysis Results for Hindcast 1957-2023, Storm Peaks and GEV Fit – Port Kembla

B.6 Batemans Bay

Extreme Value Analysis - GEV fit **Date Range** **Measured: 1986 - 2023** refer to Table 2.3
Location **Batemans Bay** **Hindcast: 1957 - 2023**

Extreme Value Analysis - Omnidirectional

ARI (years)	Dataset					
	Hindcast		Measured		Hindcast Concurrent	
	Hm0 (m)	CI (± m)	Hm0 (m)	CI (± m)	Hm0 (m)	CI (± m)
1			5.29	0.05		
2	5.88	0.12	5.74	0.19	5.76	0.14
5	6.70	0.28	6.36	0.38	6.37	0.36
10	7.34	0.42	6.82	0.56	6.86	0.55
20	8.00	0.58	7.29	0.78	7.36	0.76
50	8.88	0.81	7.91	1.10	8.05	1.06
100	9.56	1.00	8.39	1.36	8.59	1.30
200	10.25	1.20	8.86	1.63	9.13	1.55
500	11.16	1.49	9.48	2.01	9.85	1.89

Extreme Value Analysis - GEV fit **Date Range** **Measured:** **2001 - 2023** refer to Table 2.3
Location **Batemans Bay** **Hindcast:** **1957 - 2023**

Extreme Value Analysis - North-East Directional Sector (0 - 90 degrees)

ARI (years)	Dataset					
	Hindcast		Measured		Hindcast Concurrent	
	Hm0 (m)	CI (± m)	Hm0 (m)	CI (± m)	Hm0 (m)	CI (± m)
1	3.77	0.11	3.44	0.08	3.52	0.15
2	4.47	0.26	4.03	0.36	4.16	0.40
5	5.49	0.51	4.92	0.82	5.08	0.79
10	6.30	0.73	5.64	1.24	5.82	1.13
20	7.13	0.97	6.40	1.70	6.58	1.51
50	8.27	1.33	7.43	2.37	7.60	2.05
100	9.15	1.62	8.23	2.93	8.40	2.49
200	10.05	1.93	9.05	3.52	9.21	2.95
500	11.25	2.36	10.16	4.35	10.29	3.60

Extreme Value Analysis - East Southeast Directional Sector (90 - 135 degrees)

ARI (years)	Dataset					
	Hindcast		Measured		Hindcast Concurrent	
	Hm0 (m)	CI (± m)	Hm0 (m)	CI (± m)	Hm0 (m)	CI (± m)
1	4.39	0.16	4.49	0.32	4.33	0.33
2	5.20	0.31	5.09	0.34	5.00	0.41
5	6.25	0.54	5.86	0.45	5.80	0.44
10	7.03	0.77	6.44	0.69	6.36	0.54
20	7.80	1.02	7.01	0.99	6.90	0.73
50	8.82	1.38	7.75	1.45	7.58	1.08
100	9.58	1.68	8.32	1.83	8.09	1.39
200	10.34	1.99	8.88	2.22	8.58	1.73
500	11.34	2.43	9.61	2.77	9.22	2.21

Extreme Value Analysis - South Directional Sector (135 - 225 degrees)

ARI (years)	Dataset					
	Hindcast		Measured		Hindcast Concurrent	
	Hm0 (m)	CI (± m)	Hm0 (m)	CI (± m)	Hm0 (m)	CI (± m)
1	4.77	0.12	5.18	0.21	4.86	0.16
2	5.34	0.22	5.69	0.28	5.39	0.26
5	6.09	0.39	6.35	0.42	6.11	0.41
10	6.67	0.53	6.84	0.55	6.67	0.54
20	7.25	0.68	7.33	0.69	7.24	0.68
50	8.02	0.90	7.96	0.92	8.00	0.90
100	8.60	1.07	8.44	1.10	8.58	1.07
200	9.18	1.25	8.91	1.29	9.17	1.25
500	9.95	1.50	9.53	1.55	9.95	1.51

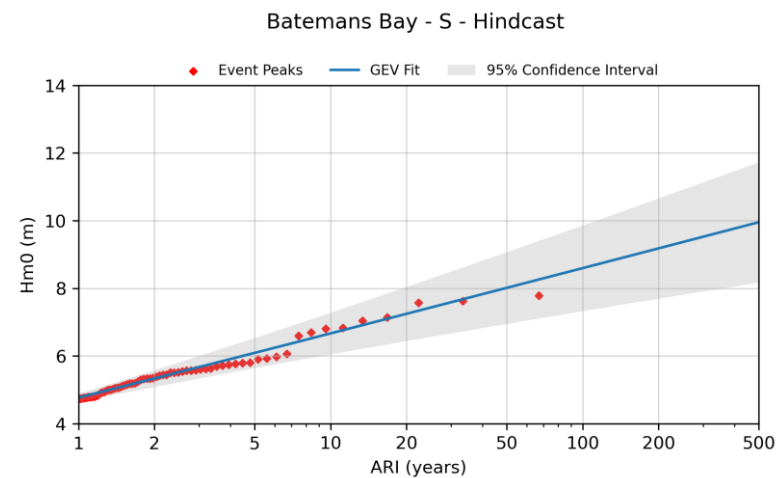
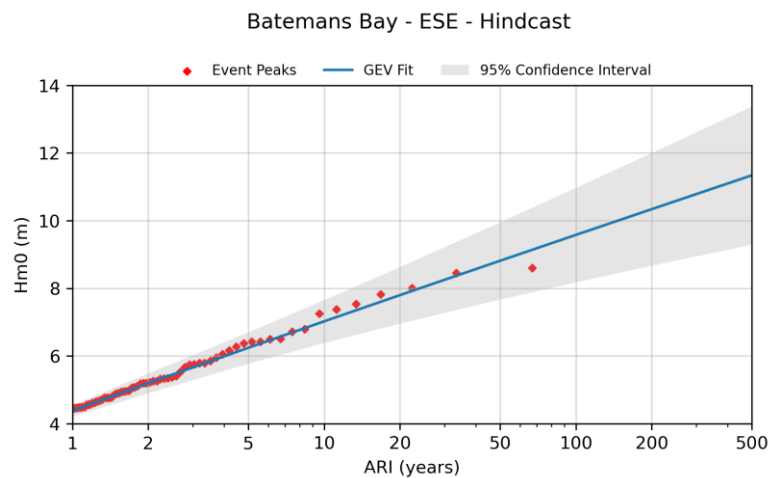
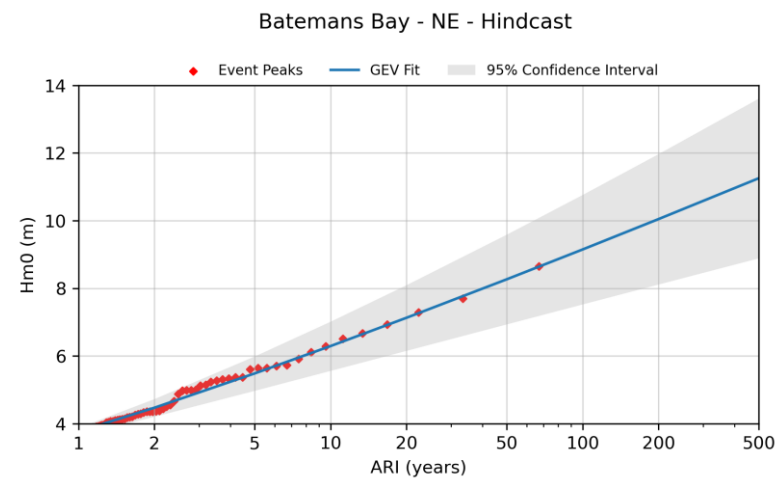
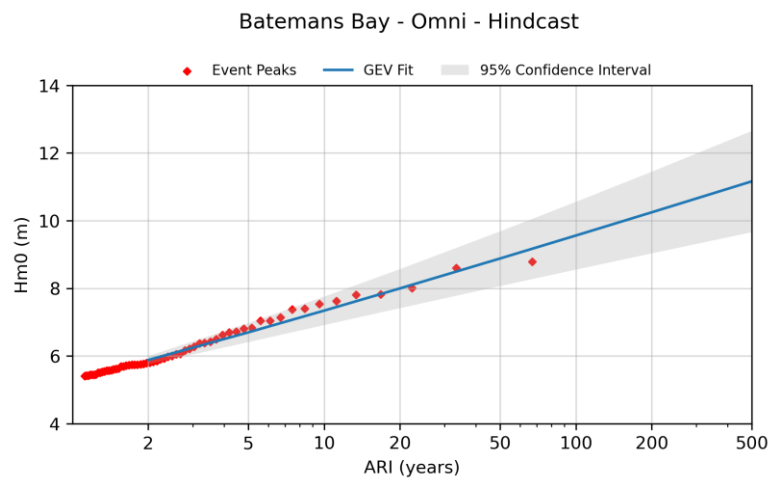


Figure B.6: Extreme Wave Height Analysis Results for Hindcast 1957-2023, Storm Peaks and GEV Fit – Batemans Bay

B.7 Eden

Extreme Value Analysis - GEV fit **Date Range** **Measured: 1985 - 2023** refer to Table 2.3
Location **Eden** **Hindcast: 1957 - 2023**

Extreme Value Analysis - Omnidirectional

ARI (years)	Dataset					
	Hindcast		Measured		Hindcast Concurrent	
	Hm0 (m)	CI (± m)	Hm0 (m)	CI (± m)	Hm0 (m)	CI (± m)
1	5.80	0.14	5.93	0.23	5.78	0.19
2	6.43	0.26	6.50	0.38	6.33	0.29
5	7.28	0.45	7.26	0.61	7.03	0.46
10	7.92	0.61	7.83	0.80	7.56	0.61
20	8.57	0.78	8.40	1.01	8.08	0.77
50	9.42	1.03	9.16	1.31	8.77	1.01
100	10.07	1.22	9.72	1.55	9.28	1.19
200	10.72	1.43	10.29	1.80	9.79	1.39
500	11.57	1.71	11.04	2.14	10.46	1.66

Extreme Value Analysis - GEV fit **Date Range** **Measured: 2011 - 2023** refer to Table 2.3
Location **Eden** **Hindcast: 1957 - 2023**

Extreme Value Analysis - North-East Directional Sector (0 - 90 degrees)

ARI (years)	Dataset					
	Hindcast		Measured		Hindcast Concurrent	
	Hm0 (m)	CI (± m)	Hm0 (m)	CI (± m)	Hm0 (m)	CI (± m)
1	4.27	0.07	4.24	0.23	4.48	20.87
2	5.08	0.24	4.81	0.82	5.38	0.66
5	6.19	0.48	6.15	1.84	6.65	0.82
10	7.04	0.68	7.55	2.83	7.63	1.06
20	7.90	0.90	9.24	4.01	8.63	1.40
50	9.04	1.22	11.91	5.90	9.96	1.96
100	9.90	1.48	14.22	7.56	10.99	2.45
200	10.77	1.75	16.78	9.44	12.02	2.97
500	11.93	2.12	20.52	12.25	13.39	3.71

Extreme Value Analysis - East Southeast Directional Sector (90 - 135 degrees)

ARI (years)	Dataset					
	Hindcast		Measured		Hindcast Concurrent	
	Hm0 (m)	CI (± m)	Hm0 (m)	CI (± m)	Hm0 (m)	CI (± m)
1	4.34	0.04	4.81	0.33	4.20	1.99
2	5.19	0.23	5.42	0.44	4.89	0.66
5	6.39	0.46	6.29	0.76	5.84	0.72
10	7.32	0.66	6.96	1.16	6.57	0.93
20	8.27	0.88	7.65	1.63	7.31	1.30
50	9.53	1.19	8.58	2.33	8.30	1.93
100	10.50	1.44	9.29	2.90	9.05	2.49
200	11.48	1.71	10.01	3.51	9.81	3.08
500	12.78	2.09	10.97	4.35	10.82	3.92

Extreme Value Analysis - South Directional Sector (135 - 225 degrees)

ARI (years)	Dataset					
	Hindcast		Measured		Hindcast Concurrent	
	Hm0 (m)	CI (± m)	Hm0 (m)	CI (± m)	Hm0 (m)	CI (± m)
1	5.80	0.15	5.80	0.35	6.02	0.29
2	6.38	0.28	6.46	0.54	6.49	0.48
5	7.14	0.48	7.33	0.99	7.09	0.78
10	7.72	0.65	8.01	1.41	7.53	1.05
20	8.30	0.84	8.68	1.88	7.97	1.33
50	9.06	1.10	9.58	2.54	8.54	1.73
100	9.64	1.30	10.27	3.08	8.96	2.05
200	10.22	1.52	10.95	3.64	9.38	2.38
500	10.99	1.81	11.86	4.40	9.93	2.83

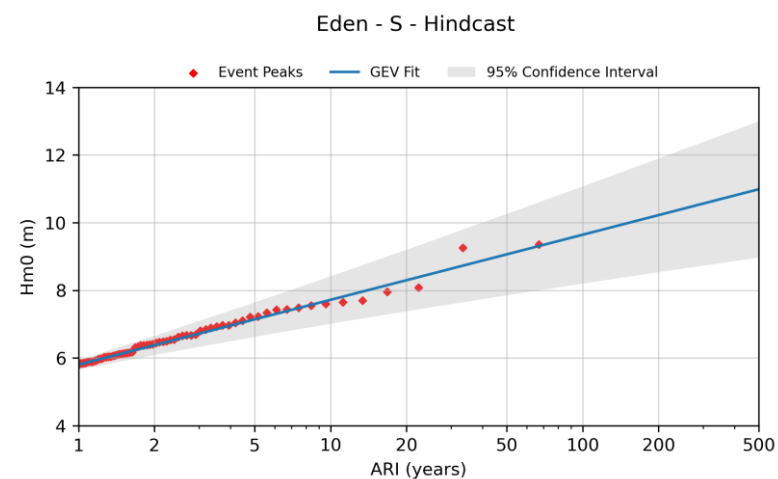
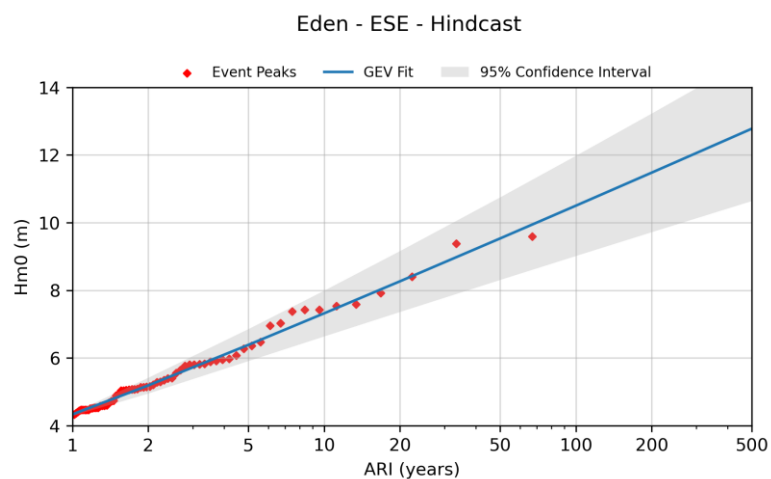
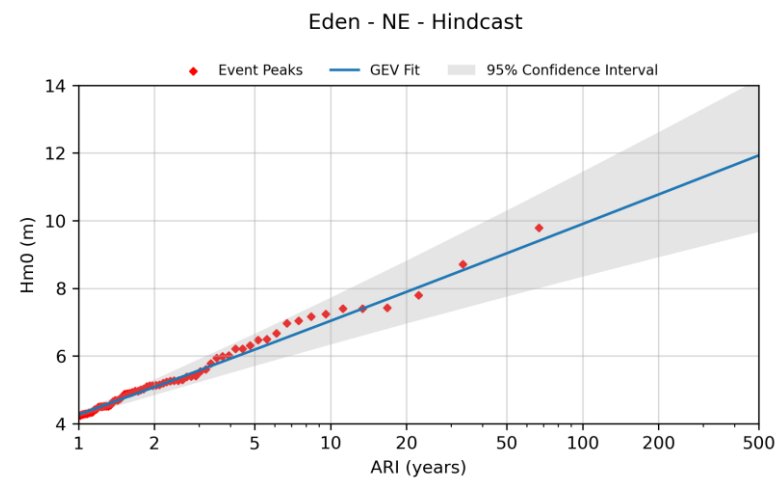
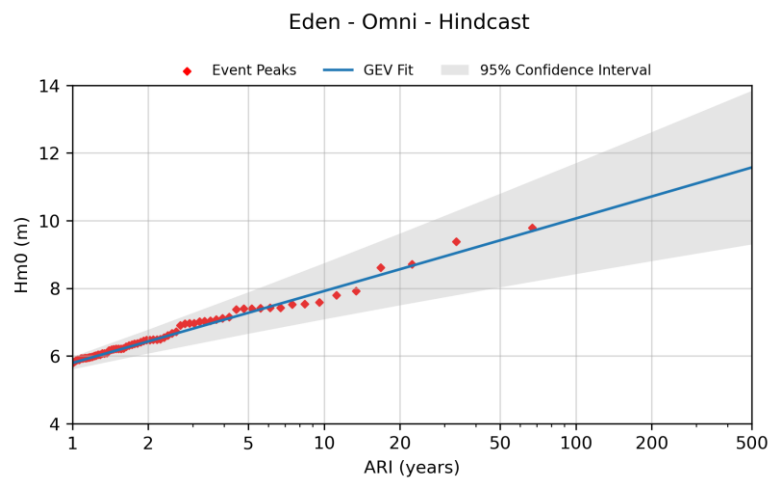
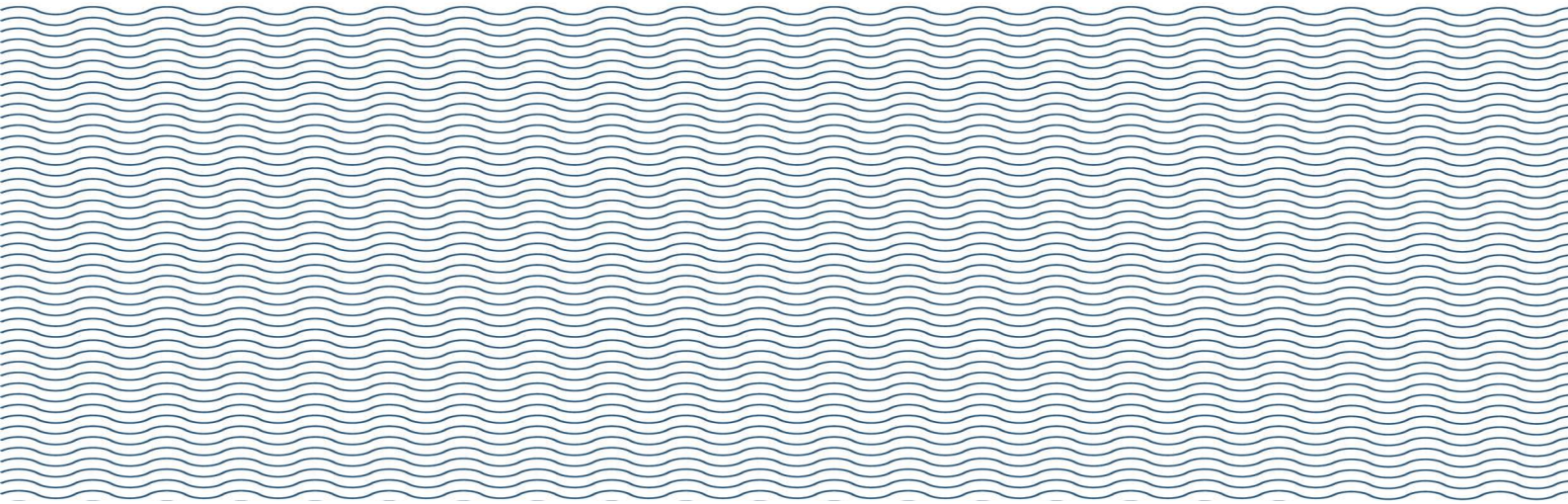


Figure B.7: Extreme Wave Height Analysis Results for Hindcast 1957-2023, Storm Peaks and GEV Fit – Eden



Appendix C

Extreme Value Distributions and Parameter Estimation

Methods (Taylor, 2006)

CHEE-824 Paper

Nonlinear Estimation of Extreme Value Model Parameters in Coastal and Ocean Engineering

Due: 28/04/2006

Abstract

Extreme Value Analysis (EVA) is an important tool utilised to develop long-term design standards when only a relatively short period of data is available. In coastal and ocean engineering, EVA is widely used to determine return periods and design levels for parameters such as wave heights, water levels and current speeds.

A range of theoretical distributions functions have been applied in EVA in coastal and ocean engineering fields including the Fisher-Tippett Type-1 (FT-I), Fisher-Tippett Type-2 (FT-II) and Weibull distributions. Functions such as the Weibull and FT-II distributions, feature parameters which are nonlinear. Traditionally, extreme value investigations using these nonlinear functions determine parameter estimates through linearization of the functions. Investigations have been undertaken into the coastal and ocean engineering application of a range of nonlinear parameter estimation techniques, including least squares and maximum likelihood approaches.

These nonlinear techniques have been applied to the investigation of two extreme wave height datasets and one extreme current speed dataset. The determination of appropriate confidence intervals through a robust bootstrap data resampling approach is also discussed.

Introduction

A critical feature in the design of any system or structure is the selection of appropriate conditions which must be accommodated. Typically infrastructure is required to remain functional during and after exposure to ambient conditions which occur on average every several decades to hundreds of years. Examples of physical forcing which have to be accommodated in civil structures include floods and wind. Determining appropriate design levels for these forcings ideally requires long-term data with a record length greater than the average return period of the design conditions. In many cases, data is not available for this length of time and design conditions have to be determined using a dataset which is significantly shorter than the average return period of the design event.

Extreme Value Analysis (EVA) is a powerful tool applied in a wide range of science and engineering fields to estimate long-return period design conditions. In coastal and ocean engineering, reliable data is at best usually only available for periods up to 50 years and EVA is applied to determine design conditions for such things as wave height, water level, current speed and wind speed.

Theoretical Development

A number of statistical functions have been applied in EVA in coastal and ocean engineering applications. Three of the most common are (Goda, 2000):-

- Fisher-Tippett Type-1 (FT-I),
- Fisher-Tippett Type-2 (FT-II), and
- Weibull distributions.

The FT-II and Weibull distributions have a non-linear parameter. Nonlinear parameter estimation approaches, including least squares and maximum likelihood techniques, have been used in the EVA of three coastal and marine datasets. These datasets are typical of those which are used to determine design conditions for coastal and marine structures. The Weibull distribution has been applied in all cases. Two datasets feature extreme wave conditions, and the third dataset features current speeds associated with tropical cyclones (hurricanes).

Weibull Distribution

The Weibull distribution has been widely applied in the investigation of long-return period events in coastal and ocean environments. In EVA, available data can be used to estimate appropriate parameters of a Weibull model, which in turn is used to determine design conditions at appropriate return intervals. Goda (2002) describes the Weibull cumulative distribution function as:-

$$F(x) = 1 - \exp\left[-\left(\frac{x-B}{A}\right)^k\right] \quad (1)$$

where A , B and k represent three parameters which have to be estimated from the available data. The A parameter is referred as the *scale parameter*, B is the *location parameter* and k is the *shape parameter*.

Parameter Estimation Techniques

Four principle techniques are described in Goda (2000) to estimate parameters. They are:-

- Graphical fitting,
- Least squares regression,
- Method of moments, and
- Maximum likelihood method.

Graphical fitting involves assembling the data in descending order and plotting the data on probability paper, for example on Weibull paper. A straight line to represent the best fit of the data is determined by visual judgement. Prior to modern computing capabilities, this method was widely used.

Least squares regression (LSR) is based on similar principles to graphical fitting. Data is assembled into descending order and assigned a plotting position. The unbiased plotting position formula for Weibull distribution described by Goda (1988) is:-

$$\begin{aligned}
 F_m &= 1 - \frac{m - \alpha}{N_T + \beta}, \quad m = 1, 2, \dots, N_T \\
 \alpha &= 0.20 + \frac{0.27}{\sqrt{k}} \\
 \beta &= 0.20 + \frac{0.23}{\sqrt{k}}
 \end{aligned} \tag{2}$$

The least squares fit is then determined by the Equations 3 and 4.

$$y_{(m)} = \left[-\ln(1 - \hat{F}_{(m)}) \right]^{\frac{1}{k}} \quad (3)$$

$$\hat{x}_{(m)} = \hat{B} + \hat{A}y_{(m)} \quad (4)$$

where \hat{F} is determined in Equation 2. In these equations, x represents the estimated value of the target response (for example wave height), and y is the reduced variate. The reduced variate is a function of the cumulative probability density function of the data.

The application of Equations 2 to 4 requires a value for k to be assumed. Through the application of nonlinear regression, \hat{A} , \hat{B} and \hat{k} can be directly solved using Equation 5. In this study, a Gauss-Newton iteration has been used to solve Equation 5.

$$\hat{x}_{(m)} = \hat{B} + \hat{A} \left[-\ln(1 - \hat{F}_{(m)}) \right]^{\frac{1}{k}} \quad (5)$$

The method of moments (MoM) is an analytical technique which was favoured when computing capacity was limited due to its relatively simple solution algorithm and low computational requirements. Goda (2000) recommends the use of least squares or maximum likelihood methods because method of moments can produce biased results.

The maximum likelihood method (MLE) is a favoured approach by statisticians due to its mathematical basis. Compared to the least squares methods, the algorithm is more complex. In these investigations, *MATLAB* has been used to determine the maximum likelihood estimates of the Weibull parameters. The Weibull likelihood function is defined in Equations 6 and 7.

$$\hat{y}_{(m)} = f\left(y \mid \hat{A}, \hat{k}\right) = \hat{k} \hat{A}^{\hat{k}} y^{\hat{k}-1} \exp\left(-\left(\frac{y}{\hat{A}}\right)^{\hat{k}}\right) I_{(0,\infty)}(y) \quad (6)$$

$$\hat{x}_{(m)} = \hat{y}_{(m)} + \hat{B} \quad (7)$$

Calculation of the optimal Weibull parameters (\hat{A} , \hat{B} and \hat{k}) requires two optimisation algorithms. \hat{A} and \hat{k} can be optimised for a specified value of B using the *MATLAB* function *wblfit.m*. A separate routine is used to calculate \hat{B} based on minimising the Mean Squared Error (MSE) of residuals. MSE is defined by Equation 8:-

$$s_{residuals}^2 = MSE = \frac{\sum_{i=1}^N (x_i - \hat{x}_i)^2}{N - p} \quad (8)$$

where x_i is the input data, \hat{x}_i is the MLE fitted data value (Equation 7), N is the sample size and p is the number of parameters (3).

Compared to the least squares parameter estimate method, the maximum likelihood method does not require a plotting position to be assigned to each data point. As a consequence, data values which vary significantly from the general trend of the dataset have less influence on the estimated parameters. This is further described in the EVA of the Gulf of Carpentaria current speed data.

Return Value Estimate

Following the estimation of parameters for the Weibull model, return values for specified average return intervals (ARI) can be calculated using the Weibull cumulative probability function. For least squares regression, the reduced variate of the specified return period y_R , is determined by Equation 9.

$$y_R = [\ln(\lambda R)]^{\frac{1}{\hat{k}}} \quad (9)$$

where λ is the average number of events per year (based on the sample data) and R is the specified return period (years). Equation 3 is then used to determine the value of the required variable.

The return value probability for maximum likelihood method can be estimated using Equation 10.

$$p = 1 - \frac{1}{\lambda R} \quad (10)$$

The calculated value for p is then used in the *MATLAB* function *wblinv.m* to calculate the value of the required variable.

Precision of the Predicted Return Values

An important component of EVA is the estimation of the confidence intervals for the calculated return values. The general formula for the precision of a predicted value is defined in Equation 11.

$$x_{k,\alpha/2} = \hat{x}_k \pm t_{v,\alpha/2} \sqrt{s_{\hat{x}_k}^2 + s_e^2} \quad (11)$$

When the predicted values are being estimated at experimental conditions, the population variance s_e , can assumed to be zero, and all the noise is contained in the original data which can be estimated from the MSE of the fitted model. In EVA, the value of population variance is significant and cannot generally be calculated directly from the sample data. An empirical method to estimate the standard deviation of a least squares fitted Weibull model is described in Goda (1992). A full description of the empirical formulas is contained in Goda (2000).

An alternative approach recommended by Mathiesen *et al* (1994) is to estimate the population variance through resampling the original data set a large number of times. This approach is generally referred to as 'bootstrapping'. It assumes that the sample is representative of the larger population however an alternative sample from the same population could have a different composition of the same values. Bootstrapping involves randomly reassembling a dataset based on the original sample a large number of times, for example 1000. Each re-sampled dataset contains values from the original sample however the composition of the new dataset is not necessarily the same as the original. A Weibull model is then fitted to each sample using an appropriate fitting technique and the return values for the specified return intervals are determined. The confidence intervals for the return values can then be estimated from the variance of the return value for each return period. Naess and Hungnes (2002) contains a detailed description of the application of bootstrapping in EVA.

Sample Datasets

Three datasets which are typical of coastal and ocean engineering applications have been investigated using EVA. These datasets are:-

- Kodiak wave data,
- Kingston wave data,
- Gulf of Carpentaria current speed data.

The Kodiak wave data has been extensively utilised in the investigation of EVA techniques including Goda (2000), Goda (1988) and van Vledder *et al* (1993). The dataset consists of wave heights greater than 6m (H_s) over a 20-year period. The total sample size is 78. The Kodiak site is located in deepwater off the south coast of Alaska.

The Kingston wave data is based on a 15-year hindcast study of wave conditions at Breakwater Park, Kingston. The study was undertaken as part of a graduate coastal engineering design project at Queen's University in 2005. This data set is typical of wave conditions experienced at confined coastal and lake locations. Both the Kodiak and Kingston wave data have been censored from the whole population using a peaks-over-threshold method. In both datasets, the minimum data values are approximately 50% of the peak value. All events in the datasets are independent.

The Gulf of Carpentaria dataset features hindcast peak current speeds during cyclone events over a 30-year period. The dataset composes 14 samples and compared to the previous datasets, the variation between the highest and second highest data values is very significant. The Gulf of Carpentaria is a shallow stretch of water in northern Australia. On average, one cyclone transits this area every two years. The storm surge associated with the cyclones can generate very strong currents which are significantly stronger than the normal tidal currents. Appendix A contains the three datasets.

Long period return values for each dataset has been investigated using nonlinear least squares regression and maximum likelihood techniques. Confidence intervals of the return values have been estimated by bootstrap resampling and the empirical formulas of Goda (2000).

Kodiak Wave Data

Table 1 details the estimates of the Weibull parameters from the least squares and maximum likelihood estimation routines. Table 2 compares the return values and confidence intervals for least squares and maximum likelihood estimated Weibull models of the Kodiak data. The least squares confidence intervals have been estimated by Goda's formula and bootstrapping.

Table 1: Weibull parameter estimates for Kodiak wave data.

Parameter	LSR	MLE
\hat{B}	5.763	5.848
\hat{A}	1.899	1.800
\hat{k}	1.423	1.383

Table 2: Return value and confidence intervals – Kodiak wave data.

Return Period (Yr)	LSR	Goda		Bootstrapping		MLE	Bootstrapping	
	Wave Height H_s (m)	95% Conf Int - Lower	95% Conf Int - Upper	95% Conf Int - Lower	95% Conf Int - Upper	Wave Height H_s (m)	95% Conf Int - Lower	95% Conf Int - Upper
5	9.84	9.10	10.58	9.21	10.48	9.80	9.18	10.42
10	10.49	9.62	11.36	9.71	11.28	10.45	9.68	11.22
20	11.10	10.12	12.09	10.14	12.07	11.06	10.12	12.01
50	11.87	10.73	13.02	10.65	13.09	11.84	10.63	13.04
100	12.43	11.17	13.68	11.00	13.85	12.40	10.98	13.81
200	12.96	11.60	14.33	11.32	14.60	12.94	11.31	14.56
500	13.64	12.14	15.15	11.71	15.58	13.63	11.71	15.55

Tables 1 and 2 indicates that there is very little difference between the least squares and maximum likelihood fitted models. Although the fitted parameters vary between the fitting techniques, the calculated return values show very little variation. This result is expected because this particular dataset is well described by a Weibull distribution. Figures 1 and 2 show the graphical diagnostics for the least squares and maximum likelihood Weibull models. The confidence limits have been described using the bootstrapping approach.

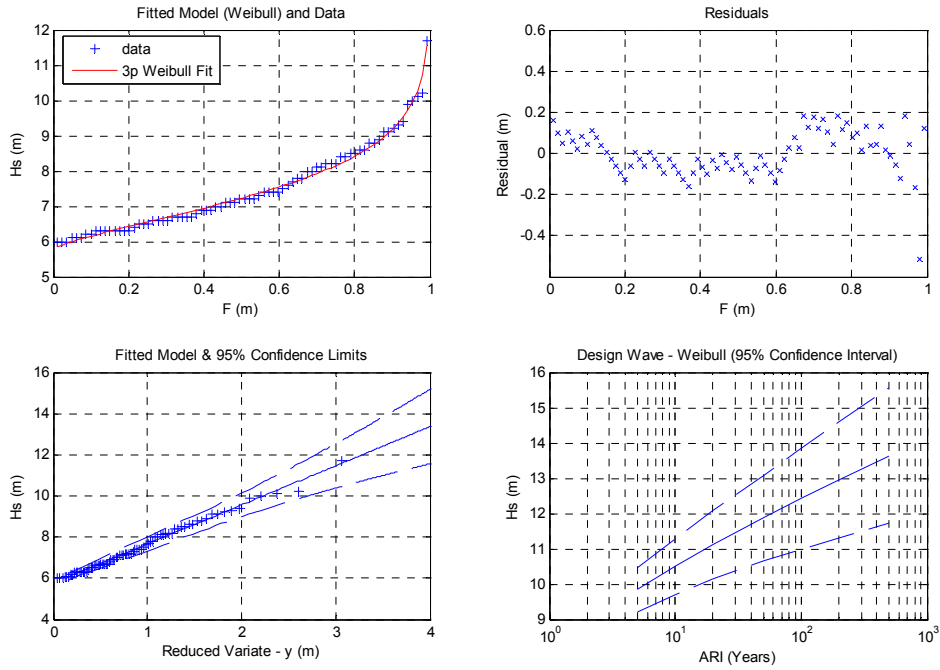


Figure 1: Graphical diagnostics of least squares fitted Weibull model – Kodiak data.

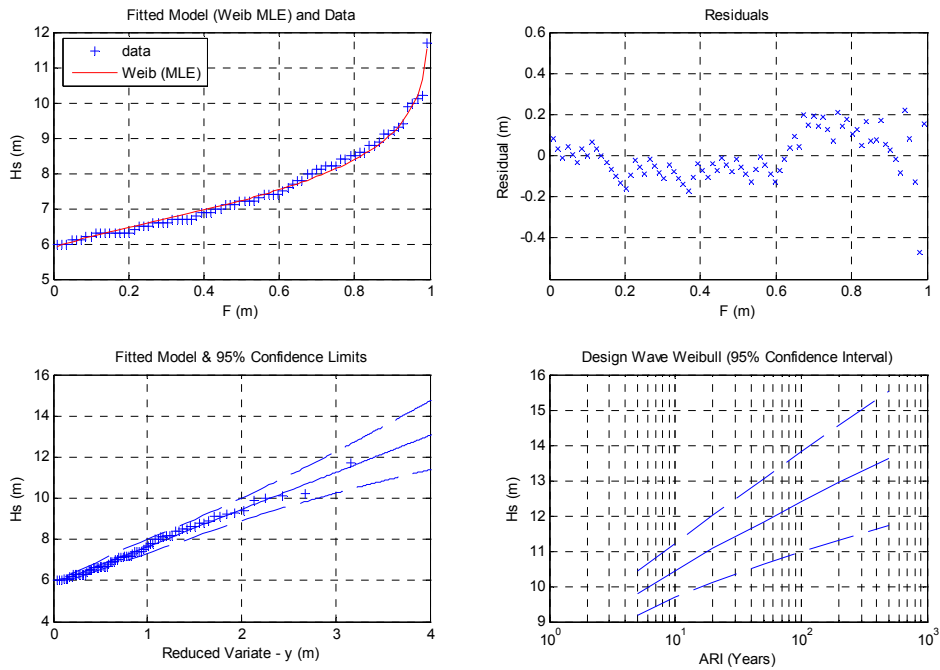


Figure 2: Graphical diagnostics of maximum likelihood fitted Weibull model – Kodiak data.

In Figures 1 and 2, the upper two plots have cumulative probability on the x-axis. The lower-left plot has the reduced variate (Equation 4) on the x-axis and the lower-right plot has average return period (ARI) on the x-axis. The overall fit of the model and the residual trend are very similar for both parameter estimation techniques. The bootstrapping technique produce wider confidence intervals for larger return period events compared to Goda's formula's.

Kingston Wave Data

Table 3 details the estimates of the Weibull parameters from the least squares and maximum likelihood estimation routines. Table 4 compares the return values and confidence intervals for least squares and maximum likelihood estimated Weibull models of the Kingston data. The least squares confidence intervals have been estimated by Goda's formula and bootstrapping.

Table 3: Weibull parameter estimates for Kingston wave data.

Parameter	LSR	MLE
\hat{B}	0.747	0.764
\hat{A}	0.286	0.267
\hat{k}	1.250	1.220

Table 4: Return value and confidence intervals – Kingston wave data.

Return Period (Yr)	LSR	Goda		Bootstrapping		MLE	Bootstrapping	
	Wave Height H_s (m)	95% Conf Int - Lower	95% Conf Int - Upper	95% Conf Int - Lower	95% Conf Int - Upper	Wave Height H_s (m)	95% Conf Int - Lower	95% Conf Int - Upper
5	1.50	1.34	1.65	1.40	1.60	1.48	1.38	1.58
10	1.62	1.44	1.80	1.51	1.72	1.60	1.49	1.71
20	1.74	1.53	1.95	1.62	1.85	1.72	1.61	1.83
50	1.89	1.64	2.13	1.76	2.01	1.87	1.74	1.99
100	2.00	1.73	2.27	1.86	2.14	1.98	1.84	2.11
200	2.11	1.81	2.40	1.95	2.26	2.08	1.94	2.23
500	2.25	1.92	2.57	2.07	2.42	2.22	2.06	2.39

Tables 3 and 4 indicates that there is very little difference between the least squares and maximum likelihood fitted models. The fitted parameters from both fitting techniques are similar and the calculated return values show very little variation. Figures 3 and 4 show the graphical diagnostics for the least squares and maximum likelihood Weibull models. The confidence limits have been described using the bootstrapping approach.

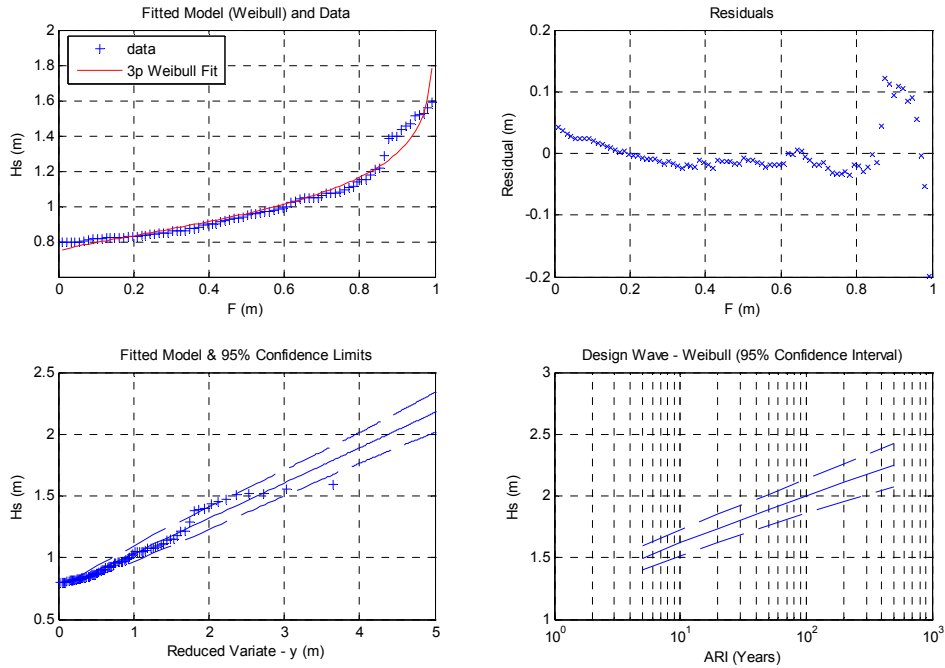


Figure 3: Graphical diagnostics of least squares fitted Weibull model – Kingston data.

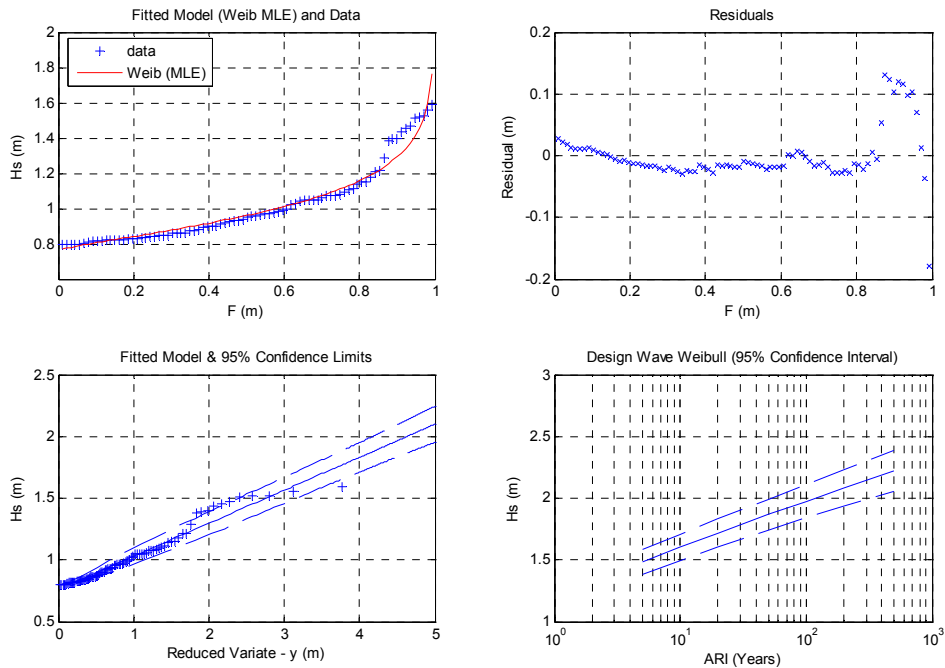


Figure 4: Graphical diagnostics of maximum likelihood fitted Weibull model – Kingston data.

The Goda's formula produced wider confidence intervals for larger return period events compared to the bootstrapping method. Compared to the Kodiak data, the Kingston data is not as well described by a Weibull distribution. Between wave heights of 1.2m to 1.5m there is a discontinuity between the cumulative probability functions of the data and the Weibull model. In the Kingston example, wave height is strongly correlated to wave direction. Consideration of wave direction, for example treating different directions as separate populations, could improve the estimation of design conditions. Wave conditions at the Kingston site are generally fetch limited, that is wave heights are limited by the length of water over which the wind forcing is acting. At this site the fetch lengths are generally less than 40km. This results in the relatively narrow and uniform confidence intervals.

The Kodiak site is exposed to wave conditions which can generate over distances of greater than 1000km. As a result, wave conditions are not influenced so much by the fetch length, but the duration of wind forcing and the overall structure of the weather systems which generate the wave conditions. This type of wave climate has a much greater variation in possible wave conditions compared to fetch limited sites.

Gulf of Carpentaria Current Speed Data

Table 5 details the estimates of the Weibull parameters from the least squares and maximum likelihood estimation routines. Table 6 compares the return values and confidence intervals for least squares and maximum likelihood estimated Weibull models of Gulf of Carpentaria current speed data. The least squares confidence intervals have been estimated by bootstrapping only because Goda's formula's do not cover the k value determined in the LSR.

Table 5: Weibull parameter estimates for Gulf of Carpentaria current speed data.

Parameter	LSR	MLE
\hat{B}	0.507	0.337
\hat{A}	0.062	0.374
\hat{k}	0.402	1.042

Table 6: Return values and confidence intervals – Gulf of Carpentaria current speed data.

	LSR	Bootstrapping		MLE	Bootstrapping	
Return Period (Yr)	Wave Height H_s (m)	95% Conf Int - Lower	95% Conf Int - Upper	Wave Height H_s (m)	95% Conf Int - Lower	95% Conf Int - Upper
5	0.55	0.36	0.73	0.66	0.50	0.82
10	0.69	0.29	1.08	0.90	0.57	1.24
20	0.96	0.33	1.59	1.15	0.58	1.71
50	1.58	0.57	2.59	1.46	0.56	2.37
100	2.27	0.83	3.70	1.70	0.52	2.88
200	3.17	1.10	5.23	1.93	0.46	3.41
500	4.71	1.35	8.08	2.24	0.36	4.13

Tables 5 and 6 indicate there is considerable variation in the estimated parameters and design conditions between the least squares and maximum likelihood parameter estimation techniques. The graphical diagnostics of the two fitting techniques illustrated in Figures 5 and 6 highlight the significant difference between the two approaches.

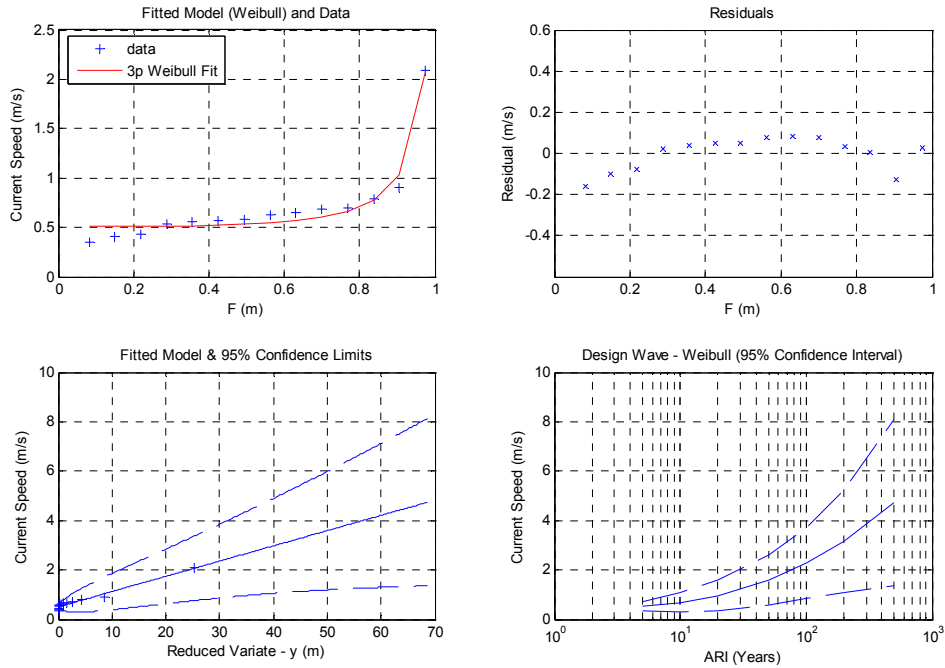


Figure 5: Graphical diagnostics of least squares fitted Weibull model – Gulf of Carpentaria current speed data.

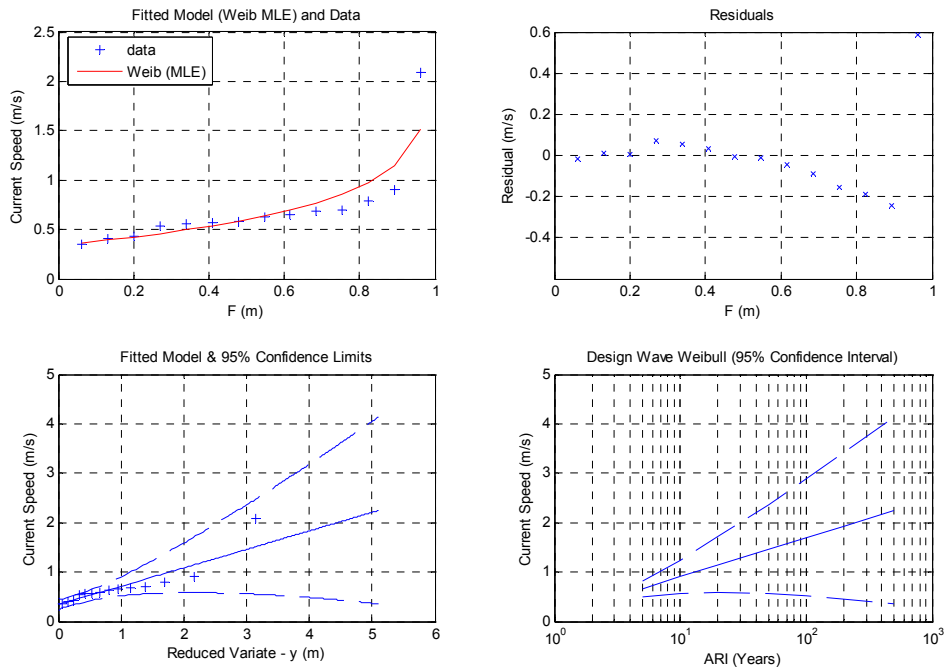


Figure 6: Graphical diagnostics of maximum likelihood fitted Weibull model – Gulf of Carpentaria current speed data.

The least squares estimation method is strongly skewed towards the relatively large magnitude of the largest data point. As a result, the design levels and confidence intervals are highly nonlinear. The maximum likelihood approach on the other hand treats the peak data point as more of an outlier and the current speed of the model at the estimated plotting position of the peak data point is significantly lower than the data value. The influence of this peak data value is accommodated in the confidence interval which on a relative basis is considerably larger than those associated with the Kingston and Kodiak wave data.

Consideration of the coefficient of correlation value, R^2 , results in the least squares model having a value of 0.982 and the maximum likelihood method having a value of 0.904. This suggests that the least squares model is the better model however this is not necessarily true. Due to the limited sample size (14 events), there is significant uncertainty in the estimation of the plotting position which is used to fit the least squares model. If a much larger sample was available covering a longer period of time, it is likely that the peak current speed of the present dataset would remain the largest value. This is because the peak current speed in the existing dataset is associated with a Category 5 tropical cyclone (Tropical Cyclone Ingrid) which resulted in the currents being concentrated at this particular location.

Tropical cyclones (hurricanes) have very large spatial gradients therefore if the path of Tropical Cyclone Ingrid varied by a few 10's of kilometres, the current speed at this site could have been significantly lower. The probability of another Category 5 tropical cyclone following a similar track to Tropical Cyclone Ingrid over next several decades to hundreds of years is relatively low.

Discussion

The EVA investigations have confirmed the suitability of the Weibull function in the description of extreme wave and current speed conditions. In the Kodiak and Kingston wave datasets, nonlinear least squares and maximum likelihood parameter estimation techniques produced very similar design wave conditions. In both these cases, the Weibull model proved to be a good description of the observed extreme wave conditions. The relatively large number of observations in each of the datasets assists in the development of a robust model which can be used to develop design conditions.

The EVA of the Gulf of Carpentaria current speed data highlighted the difference in parameter estimates which can occur between the least squares and maximum likelihood methods. This dataset was significantly different to the previous two. The total sample size was 14 and the highest current speed was significantly larger than all the other observations. The least squares regression produced a model which was a good fit of the estimated cumulative probability of the data (Figure 5) and the design current speed curve (Figure 5) is high nonlinear. The maximum likelihood parameter fitted Weibull model generally treats the largest observation point as an outlier and the estimated current speeds for design events greater than 50-Year ARI are significantly lower compared to the least squares fitted model. Based on physical understanding of cyclone (hurricane) processes, the maximum likelihood is generally a better description of the expected extreme current speed conditions at this site. The least squares parameter estimation method is dependant on a reasonable estimate of the cumulative probability description of the observed data. It is likely that the Category 5 cyclone which produced the peak current speed in the dataset has a return period at this site much greater than the 30-year period which was

investigated. If 50 to 100 years of data were available for this site, it is likely that the peak current speed of the existing dataset would remain the highest value.

The hybrid maximum likelihood algorithm which was developed in this study proved to be stable and robust. No modification of the algorithm was required to analyse all three datasets. The algorithm chooses an initial value of B slightly lower than the minimum value in the dataset. The program then estimates the other two parameters in the inner loop using a maximum likelihood approach and the MSE is calculated. The next iteration has the value of B reduced by 0.1. Once the value of MSE gradient becomes positive, the range in which an optimal value of B lies is defined and an interval halving scheme is introduced until the minimum value of MSE is achieved. In all cases, the total number of iterations of the outer loop was between 10 to 15. Figure 7 shows a plot of the MSE as a function of B for the Kodiak data. The minimum value in this dataset was 6 and the optimal B parameters is approximately 5.848. In all three datasets, the optimal value of B was relatively close to the minimum value in the data set.

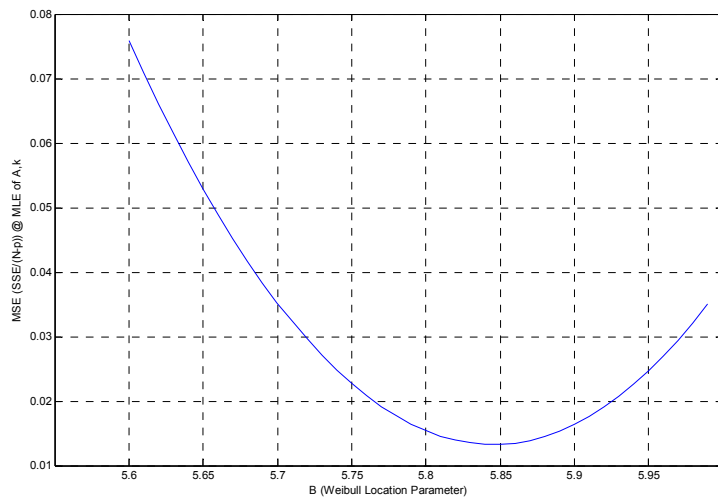


Figure 7: MSE of the maximum likelihood Weibull model as a function of B – Kodiak wave data.

The use of a bootstrap resampling method to estimate confidence levels of the design conditions has proven to be appropriate. This approach is generally similar to the approach which was used to develop Goda's empirical formula's. The advantage of the bootstrapping method used in this study is that confidence intervals for any parameter values can be developed and the confidence intervals reflect the characteristics of the individual dataset. For example, comparing extreme wave conditions at Kodiak and Kingston, due to the nature of the wave processes in the Kingston area there will be significantly less variation in the extreme wave conditions between different average return intervals at this site compared to the Kodiak site. Therefore, the relatively uniform confidence intervals developed by the bootstrapping method is consistent with this knowledge. Figure 8 highlights the why population-driven methods rather than sample-driven methods are needed to estimate confidence intervals. The outer dashed lines represent the bootstrap resampling 95% confidence intervals, and the inner dashed lines represent the 95% confidence intervals of the predictions for the Kodiak data. It is clearly evident that the population variance is an order of magnitude greater than the sample variance.

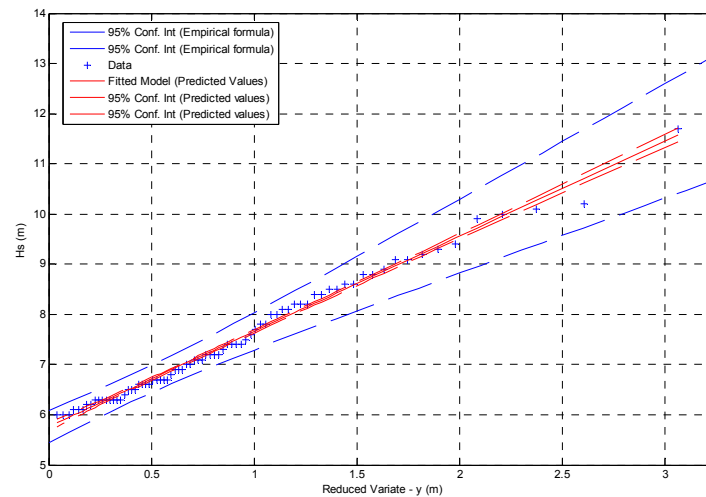


Figure 8: Comparison of the estimated 95% confidence intervals using Goda's formula and the 95% confidence intervals of predictions – Kodiak data.

Conclusions

Nonlinear least-squares and maximum likelihood methods have been developed to estimate parameters in Weibull extreme value models of coastal and ocean processes. The EVA investigations have confirmed the suitability of the Weibull function in the description of extreme wave and current speed conditions. The methods have proven to be robust and for relatively large samples (>50) which are well described by the Weibull function, both methods produce similar results.

A small extreme current speed sample which had a large degree of variance highlighted the difference in the least-squares and maximum likelihood methods. The maximum likelihood fitted model of Gulf of Carpentaria current speed data is more consistent with the expected long return period current speed conditions compared to the least squares fitted model. The maximum likelihood method is recommended when there is significant uncertainty in the estimated cumulative probability description of the dataset.

The bootstrap resampling method developed to investigate confidence intervals of design conditions proved to be an effective and robust data driven approach to estimate confidence intervals. In the case of the Kodiak data, the bootstrapping approach produced larger confidence intervals compared to Goda's empirical formulas although both methods produced confidence intervals which are similar in character. The advantage of the bootstrapping approach is the algorithm is independent of the parameters of the fitted model and unique characteristics of individual datasets can be incorporated.

References

Goda Y. (2000). "Random Seas and the Design of Maritime Structures". Advanced Series on Ocean Engineering – Volume 15. World Scientific, Singapore 2000.

Goda Y. (1988). "On the methodology of selecting design wave height." *Proceedings 21st International Conference Coastal Engineering*. pp899-913.

Goda Y. (1992). "Uncertainty of Design Parameters From Viewpoint of Extreme Statistics". *Journal of Offshore Mechanics and Arctic Engineering*. Vol 114, pp76-82, May 1992.

Gringorten I. I (1963) "A plotting rule for extreme probability paper" *Journal of Geophysical Research*. Vol 68 (3) pp 813-814.

Mathiesen M, Goda Y, Hawkes P J, Mansard E, Martin M J, Peltier E, Thompson E F and van Vledder G (1994) "Recommended Practice for Extreme Wave Analysis". *Journal of Hydraulic Research*. Vol. 32 1994 No 6.

Naess A and Hungnes B. (2002). "Estimating Confidence Intervals of Long Return Period Design Values by Bootstrapping". *Journal of Offshore and Arctic Engineering*. American Society of Mechanical Engineers.

USACE (2001) "Coastal Engineering Manual". US Army Corp of Engineers. Washington DC, 20314-1000.

van Vledder G, Goda Y, Hawkes P, Mansard E, Martin M, Mathiesen M, Thompson E F and Peltier E (1993). "Case studies of Extreme Wave Analysis: a Comparative Analysis." *Ocean Wave Measurement and Analysis – Proceedings of the Second International Symposium*. New Orleans, Louisiana.

Kodiak Wave Data

Wave Number	Height (m H_s)
1	11.7
2	10.2
3	10.1
4	10
5	9.9
6	9.4
7	9.3
8	9.2
9	9.1
10	9.1
11	8.9
12	8.8
13	8.8
14	8.6
15	8.6
16	8.5
17	8.5
18	8.4
19	8.4
20	8.2
21	8.2
22	8.2
23	8.1
24	8.1
25	8
26	8
27	7.8
28	7.8
29	7.7
30	7.6
31	7.5
32	7.4
33	7.4
34	7.4
35	7.4
36	7.3
37	7.2
38	7.2
39	7.2
40	7.2
41	7.1
42	7.1
43	7.1
44	7

Wave Number	Height (m H_s)
45	7
46	6.9
47	6.9
48	6.9
49	6.8
50	6.7
51	6.7
52	6.7
53	6.7
54	6.7
55	6.6
56	6.6
57	6.6
58	6.6
59	6.5
60	6.5
61	6.5
62	6.4
63	6.3
64	6.3
65	6.3
66	6.3
67	6.3
68	6.3
69	6.3
70	6.3
71	6.2
72	6.2
73	6.1
74	6.1
75	6.1
76	6
77	6
78	6

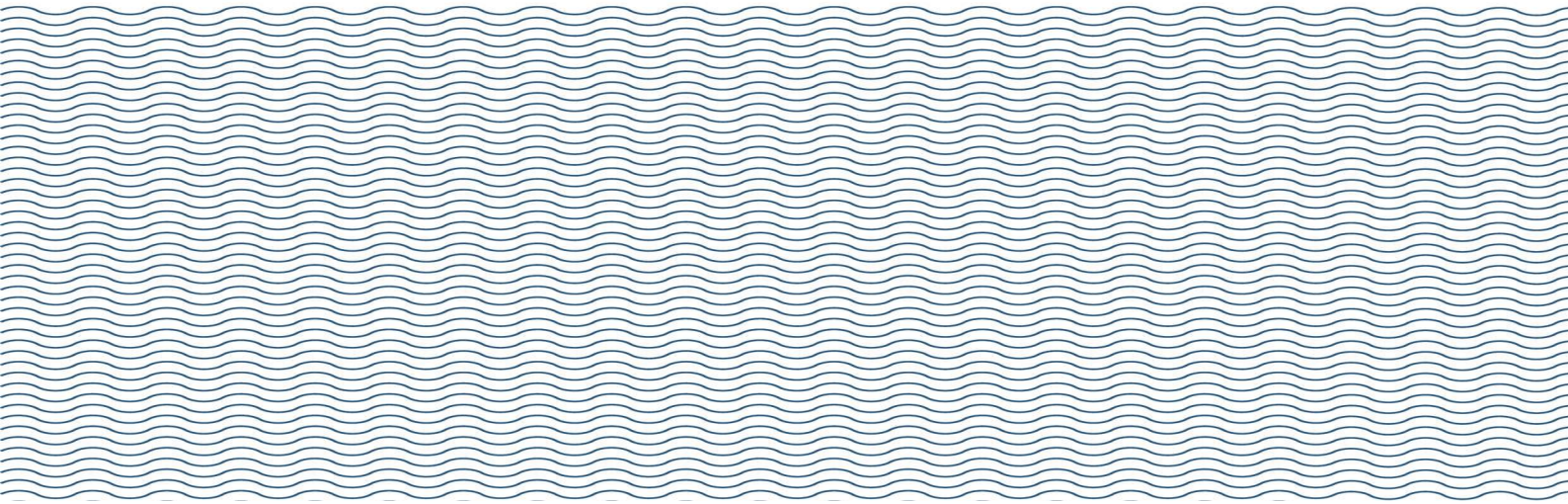
Kingston Wave Data

Wave Number	Height (m H_s)
1	1.588
2	1.559
3	1.523
4	1.522
5	1.512
6	1.469
7	1.458
8	1.436
9	1.396
10	1.394
11	1.383
12	1.288
13	1.213
14	1.21
15	1.176
16	1.154
17	1.15
18	1.14
19	1.113
20	1.107
21	1.092
22	1.082
23	1.074
24	1.073
25	1.073
26	1.061
27	1.051
28	1.05
29	1.049
30	1.049
31	1.044
32	1.03
33	1.024
34	1
35	0.991
36	0.985
37	0.979
38	0.969
39	0.968
40	0.964
41	0.961
42	0.956
43	0.953
44	0.938

Wave Number	Height (m H_s)
45	0.933
46	0.93
47	0.926
48	0.919
49	0.916
50	0.898
51	0.898
52	0.897
53	0.896
54	0.88
55	0.876
56	0.873
57	0.864
58	0.862
59	0.861
60	0.86
61	0.851
62	0.85
63	0.85
64	0.845
65	0.841
66	0.838
67	0.837
68	0.832
69	0.83
70	0.83
71	0.824
72	0.823
73	0.822
74	0.821
75	0.82
76	0.817
77	0.816
78	0.815
79	0.81
80	0.805
81	0.8
82	0.798
83	0.798
84	0.797
85	0.797

Gulf of Carpentaria Current Speed Data

Cyclone Event	Current Speed (m/s)
1	2.095
2	0.903
3	0.785
4	0.701
5	0.68
6	0.653
7	0.625
8	0.579
9	0.569
10	0.555
11	0.531
12	0.432
13	0.407
14	0.347



Appendix D

Extreme Wave Height Analysis Thresholds and Fit

Parameters



Table D.1 presents a summary of the GEV fit parameters for each site and extreme value data set (i.e. Omni-or-Directional). The GEV parameter form is as that adopted in the Matlab Statistics Toolbox for the GEV distribution (<https://au.mathworks.com/help/stats/generalized-extreme-value-distribution.html>). In Table D.1, the following parameters are specified:

- k : Shape Parameter ($k > 0$ refers to Type II EV distribution, $k = 0$ is Type 1 EV distribution, $k < 0$ refers to Type III EV distribution)
- σ : Scale Parameter
- μ : Location Parameter
- λ : Number of storm events per year in EV fit sample.
- H_{m0} thres: Specified minimum H_{m0} specified for the EV fit.
- H_{m0} min: Minimum H_{m0} in EV fit sample.

Table D.1 Summary EVA Parameters

	Measured						Hindcast Concurrent						Hindcast						
	k	σ	μ	λ	H_{m0} thres	H_{m0} min	k	σ	μ	λ	H_{m0} thres	H_{m0} min	k	σ	μ	λ	H_{m0} thres	H_{m0} min	
Byron Bay																			
Omni	-1.02	0.56	5.56	2.29	5.00	5.01	-1.05	0.77	5.53	1.72	4.80	4.80	-1.04	0.85	5.62	1.81	4.80	4.80	
NE	-1.05	0.91	4.51	1.28	3.63	3.65	-1.11	1.03	5.05	1.16	4.10	4.12	-0.93	1.06	5.64	1.00	4.50	4.51	
ESE	-1.15	0.79	4.98	1.96	4.25	4.29	-0.76	0.67	4.88	2.32	4.00	4.00	-1.01	0.81	5.21	1.57	4.40	4.41	
S	-0.94	0.59	4.89	5.49	4.25	4.26	-0.85	0.59	4.89	4.42	4.20	4.20	-0.94	0.56	5.00	3.54	4.40	4.40	

	Measured						Hindcast Concurrent						Hindcast					
Coffs Harbour																		
Omni	-0.85	0.71	5.63	2.70	4.80	4.80	-1.00	0.73	5.84	1.27	5.10	5.11	-1.06	0.82	5.48	2.12	4.70	4.70
NE	-1.15	1.24	4.51	1.45	3.40	3.43	-1.07	1.08	4.41	1.85	3.40	3.40	-1.01	1.07	4.46	1.99	3.40	3.40
ESE	-1.08	0.68	4.46	2.41	3.80	3.83	-1.23	0.80	4.57	1.18	3.90	3.91	-1.08	1.07	4.71	2.01	3.70	3.71
S	-1.08	0.73	5.86	1.35	5.15	5.18	-1.07	0.72	5.71	1.94	5.04	5.04	-0.88	0.66	5.95	1.48	5.20	5.20
Crowdy Head																		
Omni	-1.02	0.65	6.16	1.19	5.50	5.51	-0.88	0.64	6.04	1.02	5.20	5.32	-0.85	0.66	6.00	1.27	5.20	5.22
NE	-1.26	1.06	4.76	0.81	3.80	3.92	-1.08	1.06	5.08	0.89	4.00	4.09	-1.07	0.88	5.33	0.61	4.50	4.51
ESE	-1.02	0.69	4.73	1.89	4.00	4.06	-1.12	0.75	4.68	0.73	4.00	4.01	-1.05	0.84	5.12	0.73	4.30	4.32
S	-0.81	0.55	4.88	4.96	4.20	4.21	-1.12	0.70	5.34	1.70	4.70	4.71	-1.01	0.68	5.38	1.84	4.70	4.71
Sydney																		
Omni	-0.88	0.80	6.16	2.76	5.25	5.26	-0.90	0.84	6.14	2.14	5.20	5.21	-1.01	0.90	6.34	1.82	5.45	5.45
NE	-0.91	0.89	4.54	1.03	3.55	3.56	-1.07	1.04	4.98	0.91	4.00	4.00	-1.01	0.98	4.97	1.06	4.00	4.00
ESE	-1.03	0.90	5.89	0.89	5.00	5.02	-1.03	0.95	5.55	0.57	4.60	4.62	-1.07	0.81	5.80	0.58	5.00	5.04
S	-0.96	0.83	6.10	2.63	5.20	5.23	-0.91	0.90	6.20	1.73	5.20	5.21	-0.95	0.86	6.22	1.67	5.30	5.31
Port Kembla																		



	Measured						Hindcast Concurrent						Hindcast					
Omni	-1.02	0.74	5.99	2.05	5.25	5.26	-1.03	0.68	6.21	1.09	5.50	5.54	-1.02	0.83	5.83	2.12	5.00	5.01
NE	-1.12	0.85	3.80	1.94	3.00	3.04	-1.24	1.11	4.30	2.08	3.40	3.41	-1.12	0.93	4.23	2.03	3.40	3.40
ESE	-1.14	0.75	4.26	2.48	3.60	3.60	-1.07	0.85	4.24	2.34	3.40	3.45	-1.00	0.92	4.92	1.45	4.00	4.00
S	-1.06	0.73	5.00	5.17	4.30	4.31	-1.01	0.77	4.60	6.42	3.80	3.84	-1.04	0.77	5.76	1.54	5.00	5.01
Batemans Bay																		
Omni	-1.01	0.67	5.91	1.06	5.20	5.25	-1.10	0.67	6.02	0.90	5.40	5.42	-1.07	0.89	6.25	0.90	5.40	5.42
NE	-1.14	0.93	4.12	1.23	3.30	3.30	-1.11	1.01	4.32	1.40	3.40	3.42	-1.13	1.05	4.33	1.66	3.40	3.40
ESE	-0.96	0.86	4.91	1.68	4.00	4.01	-0.84	0.93	4.89	1.53	3.80	3.80	-0.97	1.16	5.10	1.48	3.90	3.91
S	-0.94	0.76	5.01	3.40	4.20	4.20	-1.06	0.76	5.01	2.23	4.30	4.30	-1.02	0.82	5.00	2.04	4.20	4.20
Eden																		
Omni	-0.99	0.84	5.85	2.97	5.00	5.00	-0.95	0.80	5.66	3.15	4.80	4.82	-1.01	0.91	5.90	2.42	5.00	5.00
NE	-1.71	1.13	4.81	1.35	4.10	4.15	-1.05	1.36	5.59	1.16	4.10	4.30	-1.03	1.20	5.27	1.16	4.10	4.10
ESE	-1.08	0.91	5.36	1.45	4.50	4.52	-1.04	1.02	4.98	1.25	4.00	4.00	-1.05	1.30	5.49	1.07	4.20	4.26
S	-1.03	0.94	6.08	2.03	5.15	5.17	-0.92	0.70	6.01	2.74	5.20	5.26	-1.00	0.83	6.03	2.07	5.20	5.20

